Food and Chemical Toxicology 125 (2019) 503–519

Contents lists available at ScienceDirect

Food and Chemical Toxicology

journal homepage: www.elsevier.com/locate/foodchemtox

Wheat phenolics suppress doxorubicin-induced cardiotoxicity via inhibition of oxidative stress, MAP kinase activation, NF-κB pathway, PI3K/Akt/mTOR impairment, and cardiac apoptosis

Ranabir Sahu[a,1], Tarun K. Dua[a], Sonjit Das[a], Vincenzo De Feo[b], Saikat Dewanjee[a,*]

[a] Advanced Pharmacognosy Research Laboratory, Department of Pharmaceutical Technology, Jadavpur University, Kolkata 700032, India
[b] Department of Pharmacy, University of Salerno, 84084 Fisciano, Salerno, Italy

ARTICLE INFO

Keywords:
Apoptosis
Cardiomyopathy
Doxorubicin
Oxidative stress
Wheat phenolics
Whole wheat grains

ABSTRACT

The present investigation has been undertaken to reveal the protective mechanism of polyphenolics extract of whole wheat grains (WWGPE), ferulic acid and apigenin against doxorubicin (Dox)-induced cardio-toxicity. WWGPE, apigenin, and ferulic acid exhibited concentration dependent cyto-protective effect against Dox (1 μM) in rat cardiomyocytes. Dox treatment significantly ($p < 0.01$) induced oxidative stress in the myocardial cells via excessive ROS production, increase in iNOS expression, NADPH oxidase activation, Nrf-2/HO-1 impairment, and inactivation of cellular redox defense system. In addition, Dox significantly ($p < 0.01$) activated MAP kinases, NF-κB, and apoptosis in cardiac cells; while, significant ($p < 0.01$) impairment in PI3K/Akt/mTOR signaling was observed in Dox-treated myocardial cells. On the other hand, WWGPE, apigenin, and ferulic acid significantly ($p < 0.05$–0.01) attenuated Dox-induced redox stress and oxidative stress-mediated signal transduction in myocardial cells. WWGPE, apigenin, and ferulic acid treatment also could significantly ($p < 0.05$–0.01) reinstate Dox-mediated changes in blood parameters in rats. Histological assessments were in agreement with the biochemical findings. Results showed that, WWGPE exhibited better cardio-protective effect over ferulic acid and apigenin, which may be due to the synergy between the comprising compounds and better oral bioavailability of dietary antioxidant molecules from whole phenolic extract.

1. Introduction

Doxorubicin (Dox), an anthracycline antineoplastic agent, is one of the first line chemotherapeutic agents used against wide range malignancies, such as sarcomas, carcinomas, and haematological cancers (Chatterjee et al., 2010). However, development of cardiotoxicity has been advocated as a serious concern in Dox-chemotherapy (Chatterjee et al., 2010). Dox-induced cardiomyopathy is frequently fatal, and reveals poor prognosis (Takemura and Fujiwara, 2007). The exact mechanism of Dox-mediated cardiotoxicity is complex and somewhat unclear; however, generation of excessive oxidative free radicals, induction of myocardial apoptosis, and alteration in the signal transductions have been proposed to contribute integrally in Dox-induced cardiomyopathy (Takemura and Fujiwara, 2007). Dox has been implicated to generate excess of oxidative free radicals, such as reactive oxygen species (ROS) and reactive nitrogen species (RNS) by more than one process (Deavall et al., 2012; Bahadır et al., 2014). Dox causes ROS overproduction in mitochondria via mitochondrial NADPH oxidase-dependent electron transfer to generate anthracycline semiquinone anion, which subsequently produces superoxide anion by reducing molecular O_2 (Deavall et al., 2012). Additionally, Dox interacts with Fe (3) to generate Fe (2)-Dox free radical, which is also capable to generate ROS via reduction of molecular O_2 (Deavall et al., 2012). Besides, Dox can elicit nitric oxide (NO) production in the cardiomyocytes via activation of inducible nitric oxide synthase (iNOS) (Boo et al., 2009). NO can react with superoxide anion to form peroxynitrite, a RNS which can target several biological molecules. In addition to overproduction of oxidative free radicals, Dox further promotes oxidative stress via impediment of cellular redox defense system and alteration in the redox-sensitive signal transduction (Dewanjee et al., 2017). Activation of nuclear factor kappa B (NF-κB), and mitogen activated protein (MAP) kinase signaling within redox stressed cellular environment was found to trigger apoptosis by activating pro-apoptotic event (Dewanjee et al., 2018). Dox has been implicated to trigger cardiac apoptosis via

* Corresponding author.
E-mail address: s.dewanjee@yahoo.com (S. Dewanjee).
[1] Present address: Department of Pharmaceutical Technology, University of North Bengal, Darjeeling 734013, India.

https://doi.org/10.1016/j.fct.2019.01.034
Received 16 November 2018; Received in revised form 9 January 2019; Accepted 18 January 2019
Available online 06 February 2019
0278-6915/

activation of c-Jun N-terminal kinases (JNKs), p38, and p53 MAP kinases (Das et al., 2011). In addition to pro-apoptotic effect, NF-κB can negatively regulate nuclear factor (erythroid-derived 2)-like 2 (Nrf-2) transcription and activities. Nrf-2 plays important role in orchestrating redox defense via activation of HO-1 and endogenous antioxidant system (Wardyn et al., 2015). Impairment in PI3K/Akt/mTOR signaling has been reported to impede cell survival process and autophagy (Ogawara et al., 2002). Dysregulation in PI3K/Akt/mTOR signaling has also been implicated in Dox-induced cardiomyopathy (Yu et al., 2017). Therefore, it could be implicated that Dox develops cardiomyopathy by a complex intracellular signaling process principally governed by oxidative free radicals. Several pharmaceutical strategies have been undertaken to prevent Dox-induced cardiomyopathy; however, clinical success is yet to be achieved (Injac and Strukelj, 2008; Carvalho et al., 2014). On the other hand, many phytotherapeuticals and phytochemicals have been reported to exert prophylactic role against xenobiotic-induced oxidative stress, apoptosis, and DNA damage (Gupta et al., 2015; Injac and Strukelj, 2008; Gupta and Sharma, 2018; Das et al., 2018; Singh and Sharma, 2018). Plant phenolics have been recognized as a major class of naturally occurring antioxidant molecules, which have been implicated to accept an electron to form comparatively stable phenoxyl radicals, and thereby interrupt oxidation chain reaction within cells (Pandey and Rizvi, 2009). Besides, plant phenolics have also been revealed to trigger cellular redox defense system via boosting the activities of endogenous antioxidant molecules (Gupta and Sharma, 2017). In addition, plant phenolics have been reported to reciprocate several xenobiotic-provoked and redox sensitive pathogenic signal transductions (Sharma and Gupta, 2016; Gupta and Sharma, 2017, 2018; Gupta et al., 2017). Considering the prophylactic role of naturally occurring antioxidants against xenobiotic-mediated oxidative stress, it would be postulated that dietary antioxidants may contribute prophylactic role against Dox-mediated oxidative damage in the myocardial tissues. Therefore, present study has been undertaken to evaluate phytotherapeutic potential of polyphenolic enriched diet against Dox-induced cardio-toxicity.

Wheat is the second major cereal crop consumed by large section of human population in daily basis. A positive correlation has been implicated between the health benefits and the quantity of consumption of whole wheat grain/day (Laddomada et al., 2015). Consumption of 2–3 servings/day (~48 g) of whole wheat grains has been claimed to reduce the risk of cardiovascular disease, type 2 diabetes, and cancer (Laddomada et al., 2015). Besides nutritional values, whole wheat grain is the major source of unique health-promoting components, such as phenolic acids and flavonoids that mainly present in the bran and germ portions (Laddomada et al., 2015). Considering the protective roles of phenolic acids and flavonoids against oxidative stress, it has been aimed to evaluate possible protective role of chemically standardized total polyphenolic extract of whole wheat grains (WWGPE) against Dox-induced cardiotoxicity employing appropriate *in vitro* and *in vivo* preclinical assays. Special attention was given to explore molecular mechanism(s) behind the cardio-protective role of WWGPE. In addition, the prophylactic effect of WWGPE has been compared with ferulic acid and apigenin, which were found to be most abundant phenolic acids and flavonoids in WWGPE, respectively.

2. Materials and methods

2.1. Chemicals

Dox (98–102%), gallic acid (97.5–102.5%), chlorogenic acid (≥95%), p-hydroxybenzoic acid (99%), caffeic acid (≥98%), syringic acid (≥95%), p-coumaric acid (≥98%), vanillic acid (≥97%), sinapic acid (≥98%), ferulic acid (≥99%), quercetin (≥95%), luteolin (≥98%), and apigenin (≥97%), fetal bovine serum (FBS), Bovine serum albumin (BSA), Dulbecco's modified Eagle's medium (DMEM), Bradford reagent, and antibodies for immunoblotting were obtained from Sigma-Aldrich Chemical Company, St. Louis, USA. $(NH_4)_2SO_4$, 1-Chloro-2,4-dinitrobenzene, 2,4-dinitrophenylhydrazine, 5,5-dithiobis (2-nitrobenzoic acid), 5-thio-2-nitrobenzoic acid, CCl_3COOH, ethylene diaminetetraacetic acid, KH_2PO_4, $Na_4P_2O_7$, NaN_3, N-ethylmaleimide, nitro blue tetrazolium, phenazinemethosulphate, reduced glutathione, reduced nicotinamide adenine dinucleotide (NADH), and thiobarbituric acid were obtained from Sisco Research Laboratory, Mumbai, India. HPLC grade solvents were brought from Merck, Mumbai, India. Kits for measurement of different biochemical parameters were purchased from Span diagnostic Ltd., India.

2.2. Extraction

Phenolics were extracted following the protocol of Sahu et al. (2016) with some modification. Pulverized whole wheat grain were extracted with 70% of methanol. The crude extract was hydrolyzed with 2M NaOH and centrifuged for 15 min at 13,200 rpm at 4 °C. The supernatant was collected and the solvent was evaporated in a speed-vac concentrator (LABCONCO, USA) at 40 °C followed by lyophilization (Heto FD 3 Drywinner, USA). Lyophilized sample, WWGPE (11.9%, w/w), was suspended in tween 80 (1%) prior to *in vivo* assay, while for *in vitro* assay, WWGPE was solubilized in DMSO (resultant ≤ 0.4% DMSO in contact to cells to avoid DMSO induced cytotoxicity).

2.3. Phytochemical screening

Identification and quantification of flavonoids and phenolic acids present in WWGPE were done by RP-HPLC method using Thermo Scientific Ultimate 3000 series HPLC system equipped with Hypersil GOLD-C18 column (250 × 4.6 mm, particle size 5μ) as previously described by Sahu et al. (2016). Instrument control and data analyses were carried out using Thermo Scientific Chromeleon Datasystem 6.80 SR12 edition. HPLC assays were performed using isocratic conditions with mobile phase comprising methanol: acetonitrile: acetic acid: o-phosphoric acid: water (40:20:2:2:20) and Water: acetonitrile (80:20 v/v) with 0.1% formic acid (pH 3.0) for flavonoids and phenolic acids, respectively. Solvents were degassed by ultra-sonication (Citizon, India), followed by filtration (Borosil, India) through a 0.45 μm membrane (Pall Life science) prior to run in the column. Injection volume comprised of 10 μl from 20 μl loop. Flow rate was set to 1 ml/min. Detection of the compounds was performed using wavelengths 340 and 280 for flavonoids and phenolic acids, respectively. Peaks were identified after comparison of the retention time (R_t) of individual 'standards' and the extract.

2.4. Animals

Healthy Wistar rats (150 ± 25 g, ♂) were procured from Chakraborty Enterprise, Kolkata, India. Animals were kept in standard polypropylene cages (3 rats/cage) in the animal house of Department of Pharmaceutical Technology, Jadavpur University, India maintained with temperature (22 ± 2 °C), humidity (45 ± 5%) and 12 h light-dark cycle (Das et al., 2018). The rats were fed standard diet and water ad libitum. The experiment has been endorsed (Ref no. AEC/PHARM/1701/09/2017) by the animal ethical committee of the same institute (Reg. No.: 0367/01/C/CPCSEA, UGC, India). The principles of laboratory animal care were followed throughout the animal experiment (PHS, 2015).

2.5. In vitro bioassays

2.5.1. Isolation of cardiomyocytes

The cardiomyocytes were isolated from the immediately decapitated hearts of the experimental rats following the method described by established protocol by our group (Bhattacharjee et al., 2017). Briefly, the Wistar rats were sacrificed by cervical dislocation under CO_2

euthanasia and hearts were excised and immediately cleaned with phosphate buffered saline of pH 7.4 (PBS). The decapitated hearts were dipped into cold Ca^{2+}-free solution and the ventricular myocardial cells were harvested by retrograde perfusion with enzyme-containing solution through the aorta using Langendorff apparatus. Finally, Ca^{2+}-replication has been executed to obtain Ca^{2+}-tolerant cardiomyocytes. The isolated murine cardiomyocytes were passaged a couple of times before executing *in vitro* assays.

2.5.2. Determination of cytotoxic effect of Dox on cardiomyocytes

Concentration dependent cytotoxic effect of Dox on cardiomyocytes was determined. Briefly, cardiomyocytes (2×10^6 cells/well) were seeded into the 24-well cell culture plate and incubated at 37 °C and 5% CO_2 for 24 h to form uniform monolayer. The cardiomyocytes were exposed to Dox (0.025–1000 μM) for 24 h and the cell viability was determined employing MTT (3-(4,5-dimethylthiazolyl-2)-2, 5-diphenyltetrazolium bromide) assay (Ghosh et al., 2011). Briefly, 250 μl of MTT solution (300 mg/ml) was added to the culture medium (200 μl/well) 1 h before the end of 24 h treatment and incubated for 30 min. After incubation, supernatants were discarded, and 200 μl of DMSO was added and absorbance was measured at 570 nm and 630 nm. The differences between the absorbance and a percentage of the corresponding controls were used to express cell viability. The experiment was repeated thrice. Dox exhibited IC_{50} value of ~ 1.2 μM in murine cardiomyocytes.

2.5.3. Determination of cytoprotective role of WWGPE, ferulic acid and apigenin on Dox intoxicated cardiomyocytes

To determine *in vitro* cytoprotective effect of WWGPE, ferulic acid and apigenin on cardiomyocytes, various sets of cardiomyocytes (~2×10^6 cells/set) were exposed to DOX (1 μM) along with ferulic acid (10–100 μM) or apigenin (1–40 μM) or WWGPE (10–200 μg/ml). 1 μM of Dox is considered to be a concentration similar to that of human plasma concentrations following toxic dose of Dox (Ghosh et al., 2011). The *in vitro* concentration range of the test materials were fixed on the basis of preliminary experiments with wide range of concentration. The cell viabilities were measured employing MTT assay at different intervals up to 24 h (Ghosh et al., 2011).

2.5.4. Hoechst nuclear staining

Hoechst 33258 staining was performed following protocol of Dua et al. (2015). Briefly, cardiomyocytes (~2000 cells/well in 384-well cell culture plate) were exposed to Dox (1 μM) and Dox (1 μM) along with ferulic acid (50 μM) or apigenin (20 μM) or WWGPE (100 μg/ml) for 24 h at 37 °C and 5% CO_2. One set of untreated cardiomyocytes was kept as normal control. After 24 h, cells were fixed with paraformaldehyde (4%) in phosphate buffer saline (PBS) of pH 7.4 for 20 min. Then the cardiomyocytes were strained with Hoechst 33258 (5 μg/ml in PBS) for 20 min followed by washing with PBS. Fluorescent nuclei and nuclear pattern were noted.

2.5.5. Flow cytometric analysis

The flow cytometric analysis was performed to predict the nature of cell death. Briefly, cardiomyocytes were exposed to Dox (1 μM) and Dox (1 μM) along with along with ferulic acid (50 μM) or apigenin (20 μM) or WWGPE (100 μg/ml) for 24 h at 37 °C and 5% CO_2. One set of untreated cardiomyocytes was kept as normal control. After 24 h, different sets of cells were treated with propidium iodide (PI) and FITC-labeled annexin V for 30 min at 37 °C (Dewanjee et al., 2017). The excess of PI and annexin V was washed out and the cardiomyocytes were fixed for analyzing in a flow cytometer using FACS Calibar (Becton-Dickinson, Mountain View, USA) fortified with 488 nm argon laser light source; 515 nm band pass filter for FITC-fluorescence and 623 nm band pass filter for PI-fluorescence using Cell Quest software. The scatter plots of PI-fluorescence (y axis) vs FITC-fluorescence (x axis) were prepared for different sets of cardiomyocytes.

2.5.6. Assays for redox markers

Different sets of cardiomyocytes were exposed to Dox (1 μM) and Dox (1 μM) along with ferulic acid (50 μM) or apigenin (20 μM) or WWGPE (100 μg/ml) for 24 h at 37 °C and 5% CO_2. One set of untreated cardiomyocytes was kept as normal control. Intracellular ROS production was measured under fluorescence microscope (Olympus-1X70, Japan) by using of 2′,7′-dichlorofluorescein diacetate (DCF-DA), which quantitatively reacts with ROS and oxidized into a fluorescence dye 2′,7′-dichlorofluorescein (DCF) (Manna and Jain, 2013). The degree of lipid peroxidation was assayed by quantifying the level of thiobarbituric acid reactive substances (TBARS) as per established protocol (Fraga et al., 1988). The protein carbonylation was determined following the protocol developed by Uchida and Stadtman (1993). Briefly, the sample was incubated for 1 h after mixing with 2,4-dinitro phenyl hydrazine (0.1%) in 2 M HCl and then treated with equal volume of trichloroacetic acid (20%) followed by centrifugation. The precipitate was washed with ethanol-ethyl acetate and dissolved in 8 M guanidine hydrochloride in 133 mM tris solution containing 13 mM EDTA and the absorbance was recorded at 365 nm. The levels of the endogenous antioxidant enzymes, such as superoxide dismutase (SOD), catalase (CAT), glutathione peroxidase (GPx), glutathione-S-transferase (GST), and glutathione reductase (GR); reduced glutathione (GSH) level; and extents of lipid peroxidation and protein carbonylation were measured following methods described elsewhere (Manna et al., 2009). SOD level was measured by the inhibition (μmol) of reduction of NBT per min at 560 nm. CAT level was measured by following the decomposition of H_2O_2 at 240 nm for 10 min and CAT unit was defined as H_2O_2 consumption/min. GST level was assayed employing conjugation reaction with glutathione in the first step of mercapturic acid synthesis and was expressed as μmol of 1-chloro-2,4-dinitrobenzene conjugate formed/minute/mg of protein. GR activity was determined as the amount of enzyme, which catalyzed the oxidation of 1 μmol NADPH/min. GPx level was measured by estimating amount of enzyme, which catalyzed the conversion of 1 μmol of NADPH into $NADP^+$ per min at the absorption intensity of 340 nm. GSH level was estimated using 5,5′-dithiobis (2-nitrobenzoic acid), which forms a yellow colored complex with GSH and the absorbance was recorded at 412 nm. The absorbance vs GSH standard curve was drawn and GSH level was estimated from this standard curve. The extent of DNA fragmentation was measured by the diphenylamine reaction (Das et al., 2018). Briefly, the cells were lysed with hypotonic lysing buffer and centrifuged to separate intact and fragmented fractions. Then the pellet and the supernatant were separately precipitated with 12.5% trichloroacetic acid. The DNA precipitates were heated to 90 °C for 10 min in 5% trichloroacetic acid and quantitatively estimated with diphenylamine and expressed as percentage over control. DNA oxidation was evaluated by RP-HPLC analysis and was expressed as 7,8-hydroxy-2′-deoxyguanosine to 10^5 x 2′-deoxyguanosine ratio as described by Das et al. (2018).

2.5.7. Western blotting of signal proteins

The protein samples for specific cellular components, such as nuclear, cytosolic, and mitochondrial proteins were separated following standard sequential fractionation procedure as described by Baghirova and co-workers (Baghirova et al., 2015). The sample proteins (20 μg) were resolved in SDS-PAGE (12%) gel electrophoresis and transferred into nitrocellulose membrane following standard transfer protocol (Dua et al., 2016). The membrane was blocked for 1 h using blocking buffer comprising tris-buffered saline +0.1% tween 20 (TBST, pH 7.6) supplemented with 5% non-fat dry milk followed by washing with TBST. The membrane was subsequently incubated with primary antibody in dilution buffer comprising TBST supplemented with 5% BSA at 4 °C overnight with gentle shaking. The membrane was then washed with TBST and was treated with suitable HRP-conjugated secondary antibody in blocking buffer at 24 °C for 1 h. The blots were developed by ECL substrate (Millipore, MA, USA) for the detection protein expressions in a ChemiDoc Touch Imaging System (Bio-Rad, USA). The

densitometric analysis was performed using Image Lab software (Bio-Rad, USA). Normalization of expression was done with respect to β-actin expression. The membranes were then subjected to mild stripping using stripping buffer comprising 25 mM glycine pH 2.0 and 1% SDS to detect the expressions of other proteins in the same membrane (Das et al., 2018). The expressions of Bcl-2, Bax, Bad, cytochrome C, Apaf-1, cleaved caspase 9, cleaved caspase 3, Bid, Fas, cleaved caspase 8, total JNK, phospho-JNK (Tyr 183/Tyr 185), total p38, phospho-p38 (Tyr 180/Tyr 182), p53, phospho-IκBα (Ser 32), total IκBα, phospho−NF−κB (p65) (Ser 536), PKC-δ, PI3K, Phospho-Akt (Ser473), total Akt, phospho-mTOR (Ser 2448), total mTOR, iNOS, HO-1, and Nrf-2 were studied.

2.6. In vivo bioassay

2.6.1. Experimental design

After 2 weeks of acclimatization, the experimental Wistar rats were divided into 8 groups (n = 6) and were treated as follows:

Group 1 (normal control): Rats received distilled water containing 2% tween 80 (*p.o.*);

Group 2: Rats were treated with ferulic acid (100 mg/kg, *p.o.*);

Group 3: Rats were treated with apigenin (100 mg/kg, *p.o.*);

Group 4: Rats were treated with WWGPE (100 mg/kg, *p.o.*);

Group 5 (toxic control): Rats were treated with Dox (3 mg/kg, *i.p.*) in every alternative day of a total of 3 dosing. The cumulative dose of 9 mg/kg was reported to be equivalent to 630 mg for a 70 kg man, which is just above the threshold dose for Dox-mediated cardiotoxicity (Ghosh et al., 2011).

Group 6: Rats were treated with ferulic acid (100 mg/kg, *p.o.*) once daily for 7 consecutive days prior to Dox (3 mg/kg; *i.p.*) treatment in every alternative day for a total of 3 dosing;

Group 7: Rats were treated with apigenin (100 mg/kg, *p.o.*) once daily for 7 consecutive days prior to Dox (3 mg/kg; *i.p.*) treatment in every alternative day for a total of 3 dosing;

Group 8: Rats were treated with WWGPE (100 mg/kg, *p.o.*) once daily for 7 consecutive days prior to Dox (3 mg/kg; *i.p.*) treatment in every alternative day for a total of 3 dosing.

The experiment has been designed following established protocol (Ghosh et al., 2011). The *in vivo* optimum dose of WWGPE has been chosen on the basis of preliminary assay with limited number of animals (3/group). The *in vivo* doses of ferulic acid, apigenin, and WWGPE were kept same to compare the protective effects of comprising phenolic acid and flavonoid of maximum quantities within WWGPE with respect to total polyphenolic extract. After 7 days, the rats were fasted overnight and were sacrificed by cervical dislocation under CO_2 euthanasia. Before sacrificing, the blood samples were collected from retro-orbital venous plexus after applying tetracaine (0.5%, one drop) ophthalmic anesthetic drop to the eyes. The hearts were excised and were immediately cleaned with PBS. The excised hearts were differently processed for histological, biochemical and immunoblotting analyses. A schematic overview of the *in vivo* bioassay has been depicted in Fig. 1.

2.6.2. Estimation of haematological and serum biochemical parameters

Total erythrocyte count, haemoglobin content, and total leucocyte count were estimated using standard laboratory procedures. The levels of total cholesterol, HDL cholesterol, triglycerides, creatine kinase (CK), lactate dehydrogenase (LDH), and aspartate aminotransferase (AST) in the sera were estimated employing commercially available kits (Span Diagnostic Limited, India) following manufacturer's protocols. Troponin I and T contents were determined by ELISA kits (Kamiya Biomedical Company, USA).

2.6.3. Estimation of biochemical parameters of myocardial tissues

The excised hearts were homogenized immediately in Tris-HCl (0.01 M)-EDTA (0.001 M) buffers of pH 7.4 and centrifuged (12,000 g) at 4 °C for 30 min to obtain supernatants for biochemical analyses. The levels of TBARS, carbonylated proteins, endogenous antioxidant enzymes, GSH, DNA oxidation, DNA fragmentation, and NADPH were measured.

2.6.4. Western blotting of signal proteins

The excised hearts were subjected to sequential fractionation procedure to obtain cytosolic, mitochondrial and nuclear protein fractions (Baghirova et al., 2015). The *in vivo* expressions of Bcl-2, Bax, Bad, cytochrome C, Apaf-1, cleaved caspase 9, cleaved caspase 3, Bid, Fas, cleaved caspase 8, total JNK, phospho-JNK (Tyr 183/Tyr 185), total p38, phospho-p38 (Tyr 180/Tyr 182), p53, phospho-IκBα (Ser 32), total IκBα, phospho−NF−κB (p65) (Ser 536), PKC-δ, PI3K, Phospho-Akt (Ser473), total Akt, phospho-mTOR (Ser 2448), total mTOR, iNOS, eNOS, HO-1, and Nrf-2 in the cardiac cells were studied.

2.6.5. Histological assessment

The excised hearts from the experimental rats were immediately fixed in 10% buffered formalin and were processed for paraffin sectioning. Sections (~5 μm) were stained with hematoxylin and eosin (H & E) for studying the histology of cardiac sections (Dewanjee et al., 2013).

2.6.6. Statistical analysis

The experimental results have been analyzed by one-way ANOVA followed by Dunnett's *t*-test employing GraphPadInStat (version 3.05), GraphPad software, USA. The data have been expressed as mean ± SD and the significance was considered when $p < 0.05$.

3. Results

3.1. Phytochemical analysis

HPLC analyses of WWGPE revealed presence of phenolic acids, such as gallic acid, chlorogenic acid, p-hydroxybenzoic acid, caffeic acid, syringic acid, p-coumaric acid, vanillic acid, sinapic acid, and ferulic acid; and the flavonoids, such as quercetin, luteolin, and apigenin (Fig. 2A). The relative abundance of phenolic acids and flavonoids in WWGPE has been shown in Fig. 2B, which revealed ferulic acid and apigenin were present in highest quantities amongst identified phenolic acids and flavonoids, respectively. The structures of the compounds were depicted in (Fig. 2C).

3.2. Effect on Dox-mediated cytotoxicity, redox status, and signal transduction in vitro

3.2.1. Dose-dependent cytotoxic effect of Dox-induced in cardiomyocytes

The cytotoxic effect of Dox was assayed by incubating isolated cardiomyocytes with different concentrations of Dox for 24 h. Dox-exposed cardiomyocytes exhibited reduction of cell viability in a concentration-dependent manner (Fig. 3A). The IC_{50} value was found to be 1.2 μM (~ 1 μM) and subsequent *in vitro* studies were performed using Dox (1 μM) as toxic control.

3.2.2. Cytoprotective effects of wheat phenolics on murine cardiomyocytes

Cardiomyocytes incubated with Dox (1 μM) exhibited gradual reduction of cell viability up to 24 h of experimental duration (Fig. 3B–D). On the other hand, simultaneous incubation of cardiomyocytes with Dox (1 μM) along with ferulic acid (10–100 μM) or apigenin (1–40 μM) or WWGPE (10–200 μg/ml) significantly reciprocated Dox-mediated reduction of cell viability up to 24 h (Fig. 3B–D). However, the optimum cytoprotective concentrations of ferulic acid, apigenin, and WWGPE were found to be 50 μM, 20 μM, and 100 μg/ml, respectively. Therefore, ferulic acid (50 μM), apigenin (20 μM), and WWGPE (100 μg/ml) have been optimized for subsequent *in vitro* experiments. The cardiomyocytes incubated with ferulic acid (50 μM) or apigenin

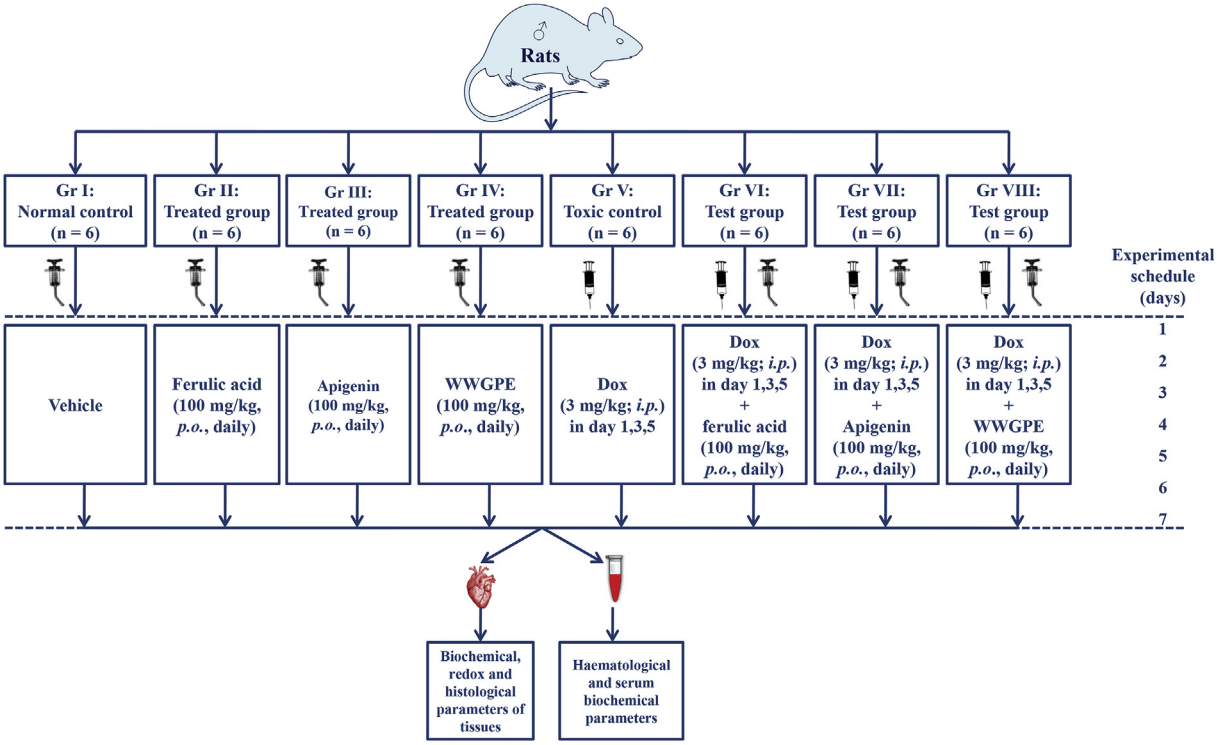

Fig. 1. A schematic overview of *in vivo* experimental protocol.

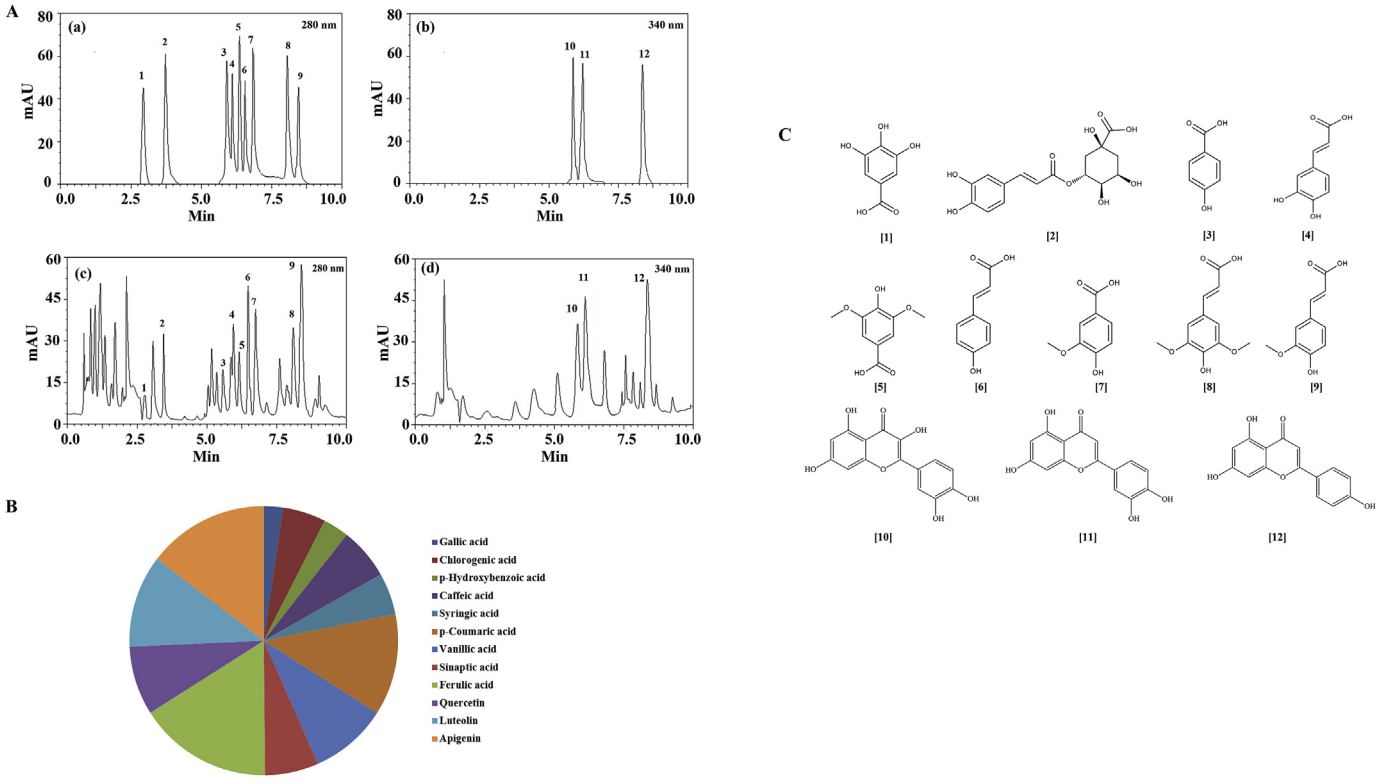

Fig. 2. A. Chromatogram of (a) standard phenolic acids, (b) standard flavonoids, (c) phenolic acids present in WWGPE, (d) flavonoids present in WWGPE. **B.** Relative abundance of phenolic acids and flavonoids in WWGPE. **C.** The chemical structures of identified phenolic acids and flavonoids. [1] gallic acid, [2] chlorogenic acid, [3] *p*-hydroxybenzoic acid, [4] caffeic acid, [5] syringic acid, [6] *p*-coumaric acid, [7] vanillic acid, [8] sinapic acid, [9] ferulic acid, [10] quercetin, [11] Luteolin, and [12] apigenin.

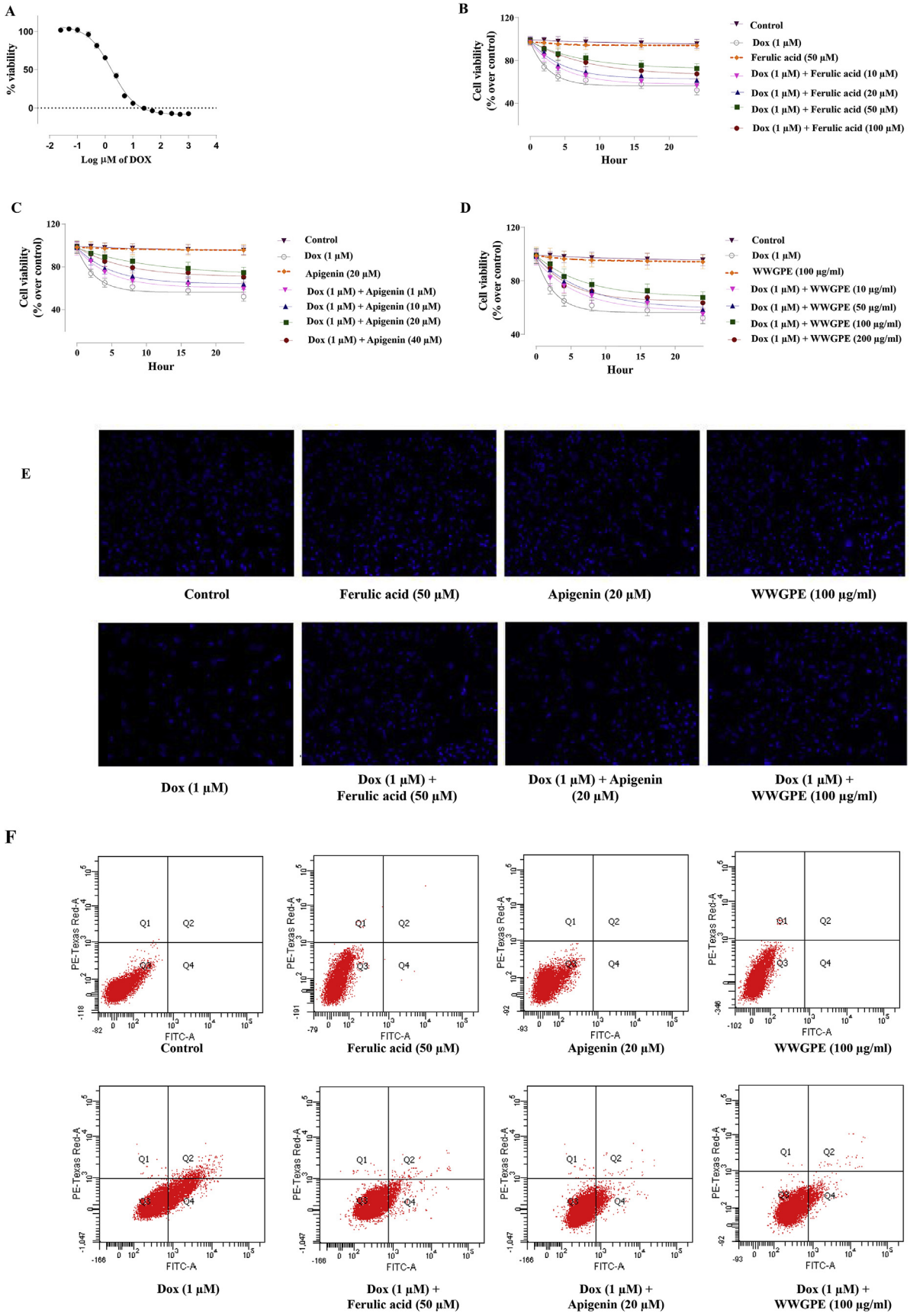

(caption on next page)

Fig. 3. The effects on cell viability, image, and flow cytometric assays in the absence (Dox) and presence of ferulic acid (Dox + ferulic acid), apigenin (Dox + apigenin), and WWGPE (Dox + WWGPE) *in vitro* in isolated rat cardiomyocytes. **(A)** Effect of Dox at different concentrations on cell viability in isolated cardiomyocytes. Data were represented as mean ± SD (n = 3). Effect on the cell viability in the absence (Dox) and presence of **(B)** ferulic acid (Dox + ferulic acid), **(C)** apigenin (Dox + apigenin), and **(D)** WWGPE (Dox + WWGPE). Data were represented as mean ± SD (n = 3). **(E)** Hoechst staining of cardiomyocytes in the absence (Dox) and presence of ferulic acid (Dox + ferulic acid), apigenin (Dox + apigenin), and WWGPE (Dox + WWGPE). **(F)** Percentage distribution of apoptotic and necrotic cells in the absence (Dox) and presence of ferulic acid (Dox + ferulic acid), apigenin (Dox + apigenin), and WWGPE (Dox + WWGPE) analyzed by flow cytometric assay.

(20 μM) or WWGPE (100 μg/ml) did not show any significant change in the cell viability when compared with untreated cardiomyocytes up to 24 h (Fig. 3B–D).

3.2.3. Effects on Hoechst staining

The cytoprotective effects of wheat phenolics were estimated by Hoechst nuclear staining following visualization through fluorescence microscope (Fig. 3E). Dox (1 μM) intoxication resulted significant reduction of visible nuclei and the nucleus exhibited explicit patterns of chromatin condensation, and fragmentation of the nuclei when compared with untreated cardiomyocytes up to 24 h. On the other hand, incubation of cardiomyocytes with Dox (1 μM) along with ferulic acid (50 μM) or apigenin (20 μM) or WWGPE (100 μg/ml) reestablished nuclear count, and restored nuclear morphology to near-normal status. Incubation of cardiomyocytes with ferulic acid (50 μM) or apigenin (20 μM) or WWGPE (100 μg/ml) for 24 h did not cause any significant change in the nuclear count or nuclear morphology when compared with untreated cardiomyocytes.

3.2.4. Flow cytometric analysis

Flow cytometric analysis revealed Dox (1 μM) treated cardiomyocytes exhibited low PI staining (~0.3%) with very high annexin V-FITC binding (~49.7%) indicating induction of apoptosis to the cardiomyocytes when compared with untreated cardiomyocytes, which showed very little annexin V-FITC binding (~0.05%), and PI staining (~0.1%) (Fig. 3F). On the other hand, incubation of cardiomyocytes with Dox (1 μM) along with ferulic acid (50 μM) or apigenin (20 μM) or WWGPE (100 μg/ml) significantly attenuated Dox-induced apoptosis in cardiomyocytes apparent for the reduction of apoptotic cell counts (Fig. 3F). Incubation of cardiomyocytes with ferulic acid (50 μM) or apigenin (20 μM) or WWGPE (100 μg/ml) for 24 h did not show any significant change in scatter plots of PI-fluorescence vs FITC-fluorescence when treated alone as compared with untreated cardiomyocytes (Fig. 3F).

3.2.5. Effects on redox status, DNA fragmentation, and DNA oxidation in vitro

Dox (1 μM)-exposed cardiomyocytes exhibited significant ($p < 0.01$) enhance in ROS production evidenced from DCF fluorescence, which subsequently promoted lipid peroxidation, and protein carbonylation (Fig. 4). Lipid peroxidation was evaluated by quantifying the level of thiobarbituric acid-reactive substances (TBARS), a by-product of lipid peroxidation. Significant ($p < 0.01$) augmentation in the levels of TBARS, and carbonylated proteins was observed in Dox (1 μM)-treated cardiomyocytes (Fig. 4). While, incubation of cardiomyocytes with Dox (1 μM) along with ferulic acid (50 μM) or apigenin (20 μM) or WWGPE (100 μg/ml) significantly ($p < 0.01$) attenuated ROS production, lipid peroxidation, and protein carbonylation (Fig. 4). Dox exposure further induced oxidative stress to the cardiomyocytes via significant ($p < 0.01$) depletion in the levels of endogenous antioxidant enzymes, and GSH (Fig. 4). On the other hand, incubation of cardiomyocytes with Dox (1 μM) along with either of ferulic acid (50 μM) or apigenin (20 μM) or WWGPE (100 μg/ml) significantly ($p < 0.05$–0.01) restored antioxidant enzymes, and GSH levels to near normal status (Fig. 4). In this study, Dox (1 μM) exposure caused significant ($p < 0.01$) fragmentation, and oxidation of DNA. On the other hand, ferulic acid (50 μM) or apigenin (20 μM) or WWGPE (100 μg/ml) significantly ($p < 0.05$–0.01) attenuate Dox-induced DNA fragmentation, and DNA oxidation in the isolated cardiomyocytes (Fig. 4). On the other hand, incubation of cardiomyocytes with ferulic acid (50 μM) or apigenin (20 μM) or WWGPE (100 μg/ml) did not show any significant change in either of aforementioned redox parameter or DNA damage when treated alone to the cardiomyocytes as compared with untreated cells (Fig. 4).

3.2.6. Effects on signal proteins in vitro

In this study, the expressions of signal proteins involved in the intrinsic and extrinsic pathways of apoptosis were assessed by western blotting (Fig. 5). Dox (1 μM) exposure caused mitochondrial translocation of pro-apoptotic Bad protein from cytosol resulting significantly ($p < 0.01$) high mitochondrial Bad to cytosolic Bad ratio. In addition, Dox-exposed cardiomyocytes exhibited significant down-regulation in the expressions of anti-apoptotic proteins, such as Bcl-2 and Bcl-xL, resulting significantly ($p < 0.01$) high mitochondrial Bad/Bcl-2 and mitochondrial Bad/Bcl-xL values. On the other hand, incubation of cardiomyocytes with Dox (1 μM) along with ferulic acid (50 μM) or apigenin (20 μM) or WWGPE (100 μg/ml) significantly ($p < 0.01$) reciprocated mitochondrial Bad/cytosolic Bad, mitochondrial Bad/Bcl-2, and mitochondrial Bad/Bcl-xL values to near-normal status. Dox exposure further promoted the release of cytochrome C into cytosol from mitochondria resulting significantly ($p < 0.01$) high cytosolic cytochrome C to mitochondrial cytochrome C ration. Simultaneous up-regulation ($p < 0.01$) of Apaf-1, and cleavages ($p < 0.01$) of caspase 9 and 3 confirmed the establishment of apoptosis in Dox-exposed cardiomyocytes. On the other hand, incubation of cardiomyocytes with Dox (1 μM) along with ferulic acid (50 μM) or apigenin (20 μM) or WWGPE (100 μg/ml) significantly inhibited cytochrome C release ($p < 0.01$) into cytosol, Apaf-1 ($p < 0.01$) up-regulation, and activation of caspase signaling ($p < 0.01$–0.05). Significant up-regulation in the expressions of FAS, Bid, and cleaved caspase 8 was observed in Dox (1 μM) ($p < 0.01$) exposed cardiomyocytes, which revealed simultaneous engrossment of the death receptor-mediated apoptosis (Fig. 5). On the other hand, incubation of cardiomyocytes with Dox (1 μM) along with ferulic acid (50 μM) or apigenin (20 μM) or WWGPE (100 μg/ml) significantly reciprocated the up-regulation of FAS ($p < 0.05$), Bid ($p < 0.01$), and cleaved caspase 8 ($p < 0.01$) expressions.

The expressions of signal proteins involved in NF-κB and MAP kinase signaling were studied (Fig. 6). Activation of NF-κB is initiated with phosphorylation mediated cleavage of NF-κB complex with inhibitory protein, IκBα. In this study, Dox (1 μM) treatment significantly ($p < 0.01$) enhanced phosphorylation of IκBα in the cytosol resulting activation of NF-κB signaling. Dox-exposed cardiomyocytes exhibited significant nuclear translocation of phospho−NF−κB (p65) from cytosol resulting significantly ($p < 0.01$) high nuclear phospho−NF−κB (p65) to cytosolic phospho−NF−κB (p65) ratio. On the other hand, incubation of cardiomyocytes with Dox (1 μM) along with ferulic acid (50 μM) or apigenin (20 μM) or WWGPE (100 μg/ml) significantly impede Dox-mediated IκBα phosphorylation ($p < 0.05$–0.01) and concomitant nuclear translocation of phospho−NF−κB (p65) ($p < 0.01$). In addition, Dox (1 μM) caused significant ($p < 0.01$) up-regulation in PKC-δ expression in cardiomyocytes, which was significantly ($p < 0.05$–0.01) reciprocated by ferulic acid (50 μM) or apigenin (20 μM) or WWGPE (100 μg/ml) treatment. Dox (1 μM) treatment also provoked MAP

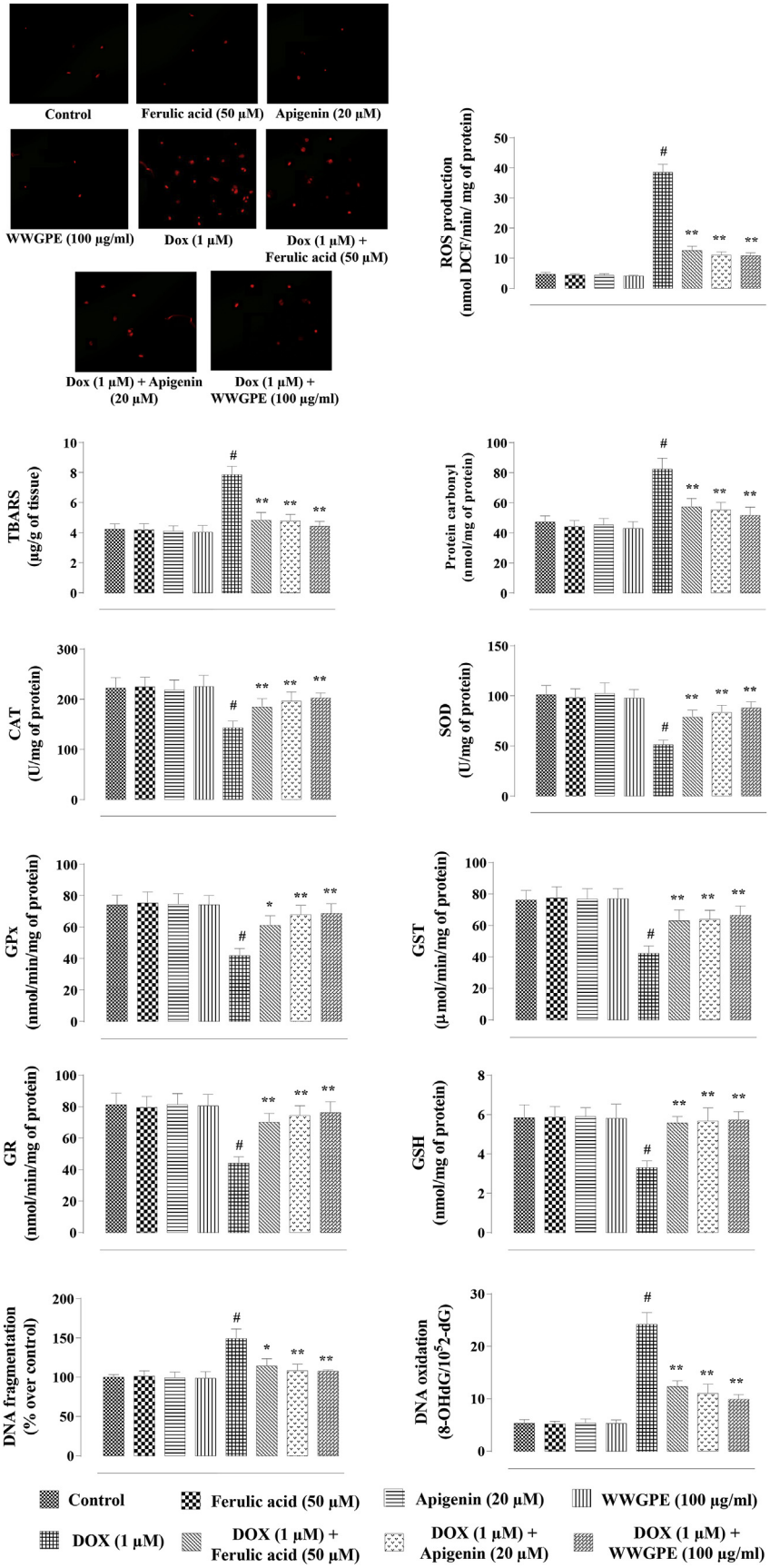

Fig. 4. The effects on ROS accumulation, lipid peroxidation, protein carbonylation, and endogenous redox systems in the absence (Dox) and presence of ferulic acid (Dox + ferulic acid), apigenin (Dox + apigenin), and WWGPE (Dox + WWGPE) in isolated rat cardiomyocytes. Data were represented as mean ± SD (n = 3). #Values significantly ($p < 0.01$) differ from normal control. *Values significantly ($p < 0.05$) differ from toxic control. **Values significantly ($p < 0.01$) differ from toxic control. SOD unit, "U", is defined as inhibition (μ moles) of NBT-reduction/min. CAT unit, "U", is defined as H_2O_2 consumption/min.

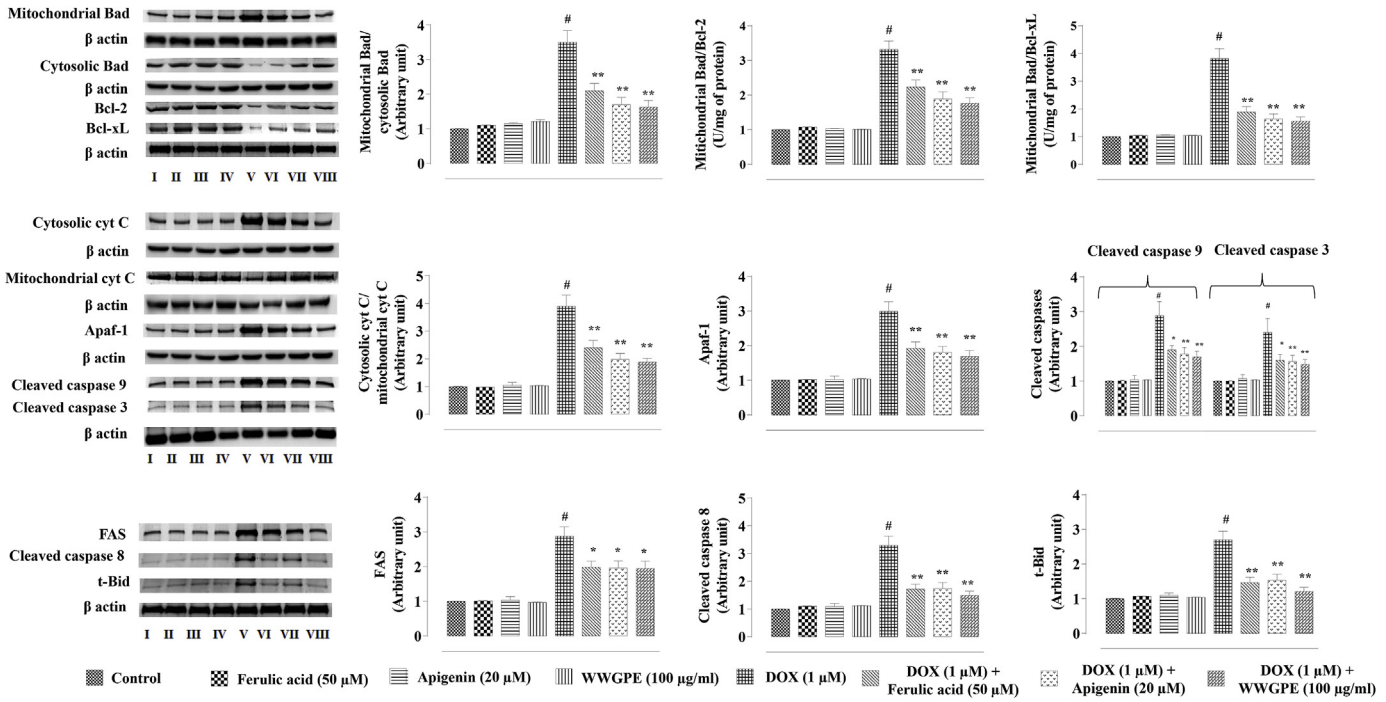

Fig. 5. The effects on intrinsic and extrinsic apoptotic signaling in the absence (Dox) and presence of ferulic acid (Dox + ferulic acid), apigenin (Dox + apigenin), and WWGPE (Dox + WWGPE) *in vitro*. The relative band intensities were assessed and the normal control band was allotted a random value of 1. β-actin served as loading control. Data were expressed as mean ± SD (n = 3). #Values significantly ($p < 0.01$) differ from normal control. *Values significantly ($p < 0.05$) differ from toxic control. **Values significantly ($p < 0.01$) differ from toxic control.

kinase signaling in cardiomyocytes evidenced from significantly ($p < 0.01$) up-regulated expressions of phospho-JNK, phospho-p38 and p53 in Dox-exposed cardiomyocytes. On the other hand, ferulic acid (50 μM) or apigenin (20 μM) or WWGPE (100 μg/ml) treatment significantly reciprocated Dox-mediated up-regulation in the phospho-JNK ($p < 0.01$), phospho-p38 ($p < 0.05$–0.01), and p53 ($p < 0.05$–0.01) expressions in the cardiomyocytes to near-normal status.

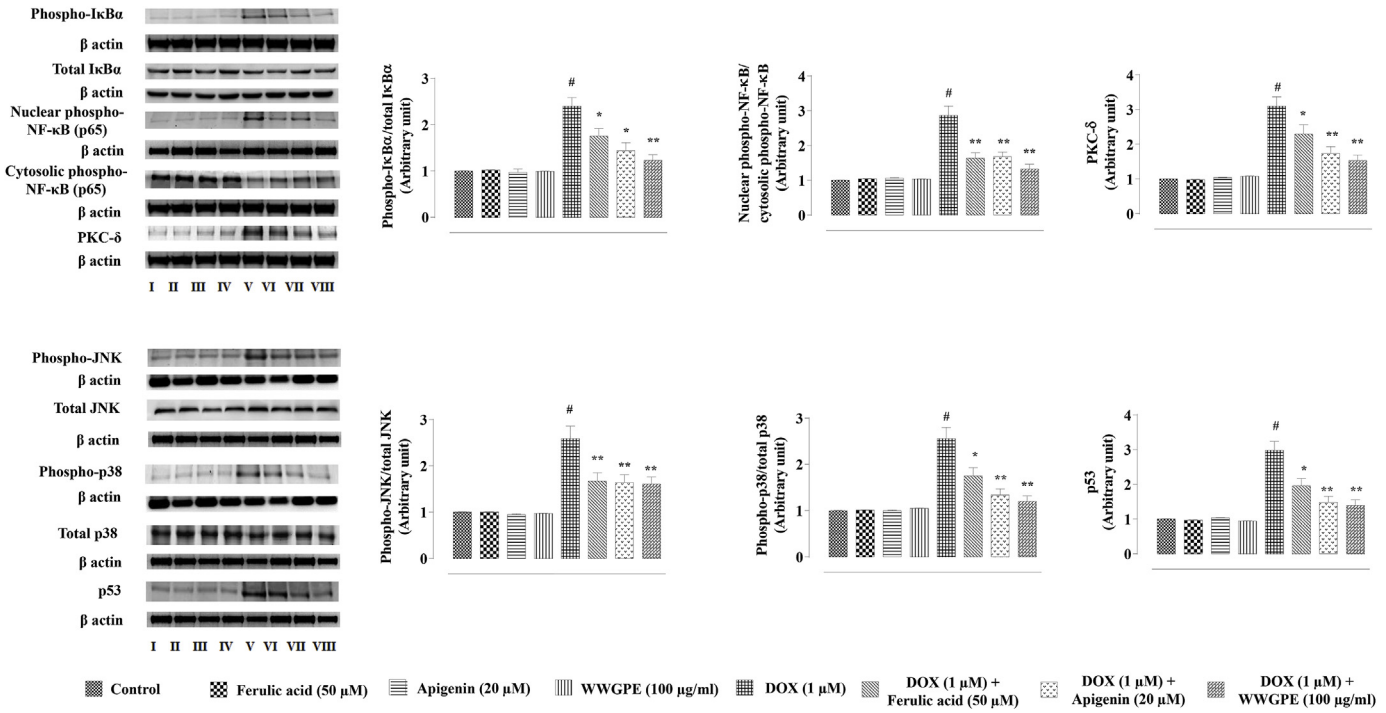

Fig. 6. The effects on IκBα, NF-κB, PKC-δ, JNK, p38, and p53 expressions in the absence (Dox) and presence of ferulic acid (Dox + ferulic acid), apigenin (Dox + apigenin), and WWGPE (Dox + WWGPE) *in vitro*. The relative band intensities were assessed and the normal control band was allotted a random value of 1. β-actin served as loading control. Data were expressed as mean ± SD (n = 3). #Values significantly ($p < 0.01$) differ from normal control. *Values significantly ($p < 0.05$) differ from toxic control. **Values significantly ($p < 0.01$) differ from toxic control.

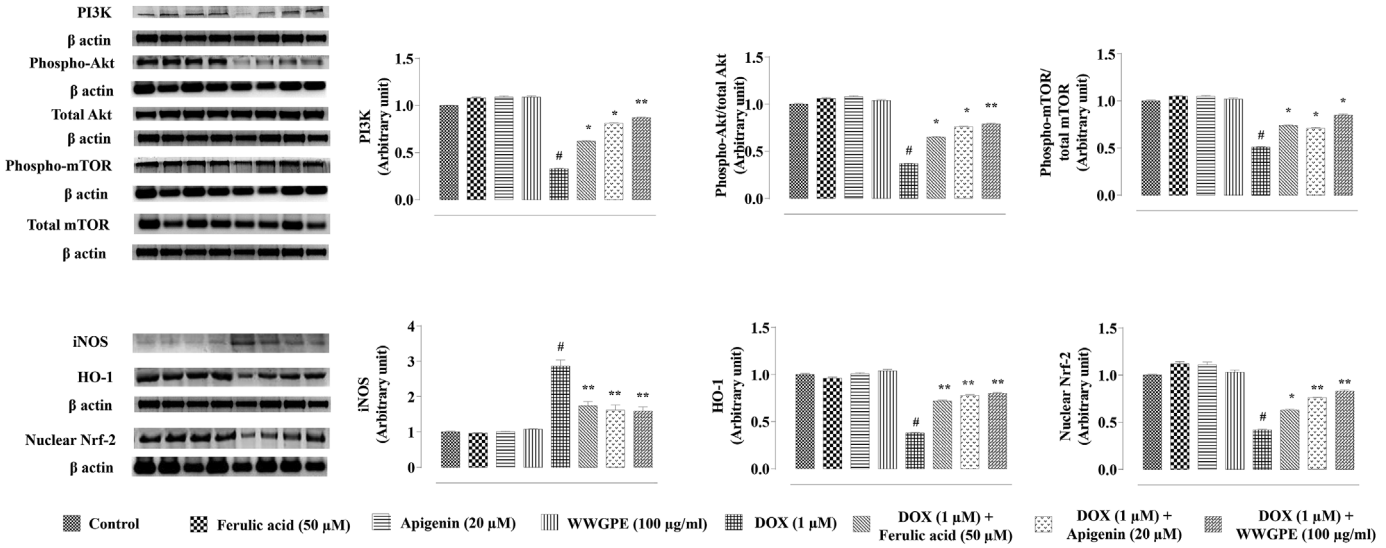

Fig. 7. The effects on PI3K, Akt, mTOR, iNOS, HO-1, and Nrf-2 expressions in the absence (Dox) and presence of ferulic acid (Dox + ferulic acid), apigenin (Dox + apigenin), and WWGPE (Dox + WWGPE) *in vitro*. The relative band intensities were assessed and the normal control band was allotted a random value of 1. β-actin served as loading control. Data were expressed as mean ± SD (n = 3). #Values significantly ($p < 0.01$) differ from normal control. *Values significantly ($p < 0.05$) differ from toxic control. **Values significantly ($p < 0.01$) differ from toxic control.

PI3K/Akt/mTOR signaling contributes in cellular survival and autophagy. Dox (1 μM) treatment significantly impaired PI3K/Akt/mTOR signaling in the cardiomyocytes evidenced from significant ($p < 0.01$) down-regulation in the expressions of PI3K, phospho-Akt and phospho-mTOR in Dox-exposed cardiomyocytes (Fig. 7). On the other hand, ferulic acid (50 μM) or apigenin (20 μM) or WWGPE (100 μg/ml) along with Dox (1 μM) significantly ($p < 0.01$) reciprocated Dox-mediated inactivation of PI3K/Akt/m-TOR signaling in the cardiomyocytes to near-normal status (Fig. 7).

To investigate role of nitric oxide (NO) in Dox-mediated cardiotoxicity, the expressions of iNOS was studied (Fig. 7). In this study, Dox (1 μM) treatment caused significant up-regulation in the expression of iNOS in cardiomyocytes. On the other hand, ferulic acid (50 μM) or apigenin (20 μM) or WWGPE (100 μg/ml) treatment could significantly ($p < 0.01$) revert Dox-provoked changes in iNOS expressions to near-normal status. In addition, Dox (1 μM) treatment significantly ($p < 0.01$) impeded HO-1 and nuclear Nrf-2 expressions; however, simultaneous incubation of ferulic acid (50 μM) or apigenin (20 μM) or WWGPE (100 μg/ml) along with Dox (1 μM) could significantly reciprocate Dox-mediated changes in HO-1 ($p < 0.01$) and nuclear Nrf-2 ($p < 0.05$–0.01) expressions to near normal status (Fig. 7).

Incubation of cardiomyocytes with ferulic acid (50 μM) or apigenin (20 μM) or WWGPE (100 μg/ml) did not show any significant change the expression of any signal protein when treated alone to the isolated cardiomyocytes as compared with untreated control set (Figs. 5–7). In *in vitro* studies, WWGPE (100 μg/ml) exhibited best protective effect over ferulic acid (50 μM) or apigenin (20 μM) against Dox-induced cardio-toxicity. The order of cardio-protective effect was found to be WWGPE (100 μg/ml) > apigenin (20 μM) > ferulic acid (50 μM) with respect to the cyto-protective parameters studied.

3.3. Effect on Dox-mediated cardiotoxicity in vivo

3.3.1. Effect on blood parameters

Haematological and serum biochemical parameters give initial imprint of pathological state within the system. The effects of wheat phenolics on blood parameters were shown in Table 1. Dox (3 mg/kg) treated rats exhibited significant ($p < 0.01$) reduction in blood cell counts and haemoglobin level. Dox (3 mg/kg) treatment significantly ($p < 0.01$) increased total cholesterol, triglycerides, AST, LDH, and CK levels in the sera of experimental rats; however, serum HDL cholesterol level was found to be decreased ($p < 0.01$) in Dox-intoxicated rats. The levels of troponins I and T in the sera are the specific markers for revealing myocardial injury. In this study, significant ($p < 0.01$) increase in the levels of troponins I and T were observed in the sera of Dox-intoxicated rats. On the other hand, oral treatment of ferulic acid (100 mg/kg) or apigenin (100 mg/kg) or WWGPE (100 mg/kg) along with Dox (3 mg/kg) significantly ($p < 0.05$–0.01) restored aforementioned haematological and serum biochemical parameters to near-normal status. Neither of ferulic acid (100 mg/kg) nor apigenin (100 mg/kg) nor WWGPE (100 mg/kg) could affect either haematological or serum biochemical parameters when treated alone to the experimental rats.

3.3.2. Effects on redox status, DNA fragmentation, and DNA oxidation in heart

Dox (3 mg/kg) treated rats exhibited significant ($p < 0.01$) increase in ROS production in myocardial cells (Fig. 8). Significant ($p < 0.01$) augmentation in the extents of lipid peroxidation, and protein carbonylation was observed in the myocardial tissue of Dox (3 mg/kg) treated rats (Fig. 8). On the other hand, oral treatment of ferulic acid (100 mg/kg) or apigenin (100 mg/kg) or WWGPE (100 mg/kg) along with Dox (3 mg/kg) significantly ($p < 0.05$–0.01) reduced myocardial ROS production, lipid peroxidation, and protein carbonylation (Fig. 8). Dox intoxication further promoted oxidative stress in the myocardial tissue via significant ($p < 0.01$) depletion of endogenous antioxidant molecules, and significant ($p < 0.01$) up-regulation of NADPH oxidase level (Fig. 8). On the other hand, oral treatment of ferulic acid (100 mg/kg) or apigenin (100 mg/kg) or WWGPE (100 mg/kg) along with Dox (3 mg/kg) significantly ($p < 0.05$–0.01) restored antioxidant enzymes, NADPH oxidase, and GSH levels to near-normal status (Fig. 8). In this study, Dox treatment significantly ($p < 0.01$) enhanced DNA fragmentation, and DNA oxidation in the cardiac tissue of experimental rats and wheat phenolics could significantly ($p < 0.05$–0.01) attenuate Dox-mediated DNA fragmentation, and DNA oxidation in the myocardial tissue of experimental rats (Fig. 8).

On the other hand, ferulic acid (100 mg/kg) or apigenin (100 mg/kg) or WWGPE (100 mg/kg) treatment did not show any significant change the expression of in redox status, DNA fragmentation, and DNA oxidation when treated alone to the experimental rats (Fig. 8).

Table 1
The effect on haematological and serum biochemical parameters in the absence (Dox) and presence of ferulic acid (Dox + ferulic acid), apigenin (Dox + apigenin), and WWGPE (Dox + WWGPE) in rats.

Parameters	Groups							
	Group I	Group II	Group III	Group IV	Group V	Group VI	Group VII	Group VIII
Total erythrocytes count ($x10^6/mm^3$)	5.67 ± 0.33	5.71 ± 0.57	5.64 ± 0.82	5.75 ± 0.67	3.73 ± 0.54$^{\#}$	4.78 ± 0.52*	4.69 ± 0.47*	5.03 ± 0.71**
Haemoglobin (g/dl)	11.07 ± 1.50	11.21 ± 1.33	11.22 ± 1.67	11.18 ± 1.41	7.81 ± 0.92$^{\#}$	10.08 ± 1.23*	9.89 ± 1.02*	10.24 ± 1.24*
Total leucocytes count ($x10^3/mm^3$)	5.23 ± 0.55	5.12 ± 0.67	5.17 ± 0.76	5.11 ± 0.72	3.61 ± 0.45$^{\#}$	4.63 ± 0.43*	4.56 ± 0.52*	4.72 ± 0.63*
Total cholesterol (mg/dl)	89.28 ± 7.37	87.43 ± 8.12	88.72 ± 9.11	87.04 ± 8.73	131.43 ± 14.50$^{\#}$	115.22 ± 10.87*	114.59 ± 9.52*	108.97 ± 11.03**
HDL cholesterol (mg/dl)	34.14 ± 3.45	34.02 ± 2.29	35.11 ± 3.94	34.96 ± 3.47	22.14 ± 2.11$^{\#}$	27.73 ± 3.05*	27.22 ± 3.01*	28.13 ± 3.12*
Triglycerides (mg/dl)	94.33 ± 9.58	93.27 ± 10.14	93.89 ± 8.92	92.55 ± 10.23	128.27 ± 12.87$^{\#}$	109.59 ± 11.28*	110.22 ± 10.15*	108.19 ± 9.35*
LDH (U/l)	173.33 ± 17.11	171.01 ± 18.33	170.44 ± 15.23	170.50 ± 17.19	225.11 ± 21.19$^{\#}$	194.89 ± 20.17*	199.22 ± 19.12*	187.76 ± 20.01*
CK (IU/mg protein)	32.04 ± 3.52	31.67 ± 3.12	33.96 ± 3.58	33.15 ± 3.47	44.14 ± 4.37$^{\#}$	37.24 ± 3.83*	38.14 ± 3.98*	36.13 ± 3.28**
AST (IU/l)	47.17 ± 5.28	47.22 ± 4.86	46.18 ± 4.91	45.77 ± 5.03	64.12 ± 7.11$^{\#}$	54.65 ± 4.98*	55.78 ± 5.17*	53.12 ± 4.51**
Troponin I (ng/ml)	1.32 ± 0.14	1.32 ± 0.29	1.33 ± 0.17	1.35 ± 0.12	2.14 ± 0.23$^{\#}$	1.82 ± 0.19*	1.79 ± 0.11*	1.72 ± 0.15**
Troponin T (pg/ml)	0.47 ± 0.05	0.46 ± 0.06	0.47 ± 0.03	0.44 ± 0.03	0.67 ± 0.08$^{\#}$	0.57 ± 0.05*	0.57 ± 0.07*	0.52 ± 0.05**

Data were represented as mean ± SD (n = 6). $^{\#}$Values significantly ($p < 0.01$) differ from normal control. *Values significantly ($p < 0.05$) differ from toxic control. **Values significantly ($p < 0.01$) differ from toxic control. Group I: Normal control; Group II: Ferulic acid (100 mg/kg); Group III: Apigenin (100 mg/kg); Group IV: WWGPE (100 mg/kg); Group V: Dox (3 mg/kg); Group VI: DOX (3 mg/kg) + Ferulic acid (100 mg/kg); Group VII: DOX (3 mg/kg) + Apigenin (100 mg/kg); Group VIII: DOX (3 mg/kg) + WWGPE (100 mg/kg).

3.3.3. Effects on signal proteins in vivo

In this study, Dox (3 mg/kg) treatment significantly promoted cytosol to mitochondrial translocation of Bad protein ensuing significantly ($p < 0.01$) high mitochondrial Bad to cytosolic Bad ratio in the myocardial cells of experimental rats (Fig. 9). Significantly down-regulation of Bcl-2 and Bcl-xL expressions was observed in the heart of Dox (3 mg/kg) treated rats (Fig. 9). Mitochondrial translocation of pro-apoptotic factor coupled with down-regulation of anti-apoptotic factors further caused cytosolic release of cytochrome C ($p < 0.01$) and activation of Apaf-1 ($p < 0.01$) in the myocardial cells of Dox (3 mg/kg) treated rats (Fig. 9). Dox (3 mg/kg) treatment further activated ($p < 0.01$) cleavage of caspase 9 and 3 (Fig. 9). On the other hand, oral treatment of ferulic acid (100 mg/kg) ($p < 0.05$–0.01) or apigenin (100 mg/kg) ($p < 0.05$) or WWGPE (100 mg/kg) ($p < 0.01$) along with Dox (3 mg/kg) significantly attenuated the intrinsic signaling of apoptosis (Fig. 9). Dox (1 μM) treatment significantly ($p < 0.01$) enhanced the expressions of FAS, Bid, and cleaved caspase 8 in the myocardial cells of experimental rats (Fig. 9). On the other hand, oral treatment of ferulic acid (100 mg/kg) or apigenin (100 mg/kg) or WWGPE (100 mg/kg) along with Dox (3 mg/kg) significantly ($p < 0.05$–0.01) attenuated the death receptor mediated apoptotic signaling (Fig. 9).

Dox (3 mg/kg) treatment significantly ($p < 0.01$) enhanced phosphorylation of IκBα and promoted nuclear translocation of phospho−NF−κB (p65) in the myocardial cells of experimental rats (Fig. 10). A significant ($p < 0.01$) activation of PKC-δ was observed in the myocardial cells of Dox-treated rats (Fig. 10). On the other hand, oral treatment of ferulic acid (100 mg/kg) or apigenin (100 mg/kg) or WWGPE (100 mg/kg) along with Dox (3 mg/kg) significantly ($p < 0.05$–0.01) impeded the NF-κB, and PKC-δ activation (Fig. 10). In addition, Dox (3 mg/kg) treatment significantly ($p < 0.01$) promoted phosphorylation of MAP kinases, such as JNK and p38 in cardiac cells of experimental rats (Fig. 10). A significant ($p < 0.01$) activation of p53 was observed in the myocardial cells of Dox-treated rats (Fig. 10). On the other hand, oral treatment of ferulic acid (100 mg/kg) or apigenin (100 mg/kg) or WWGPE (100 mg/kg) along with Dox (3 mg/kg) significantly ($p < 0.05$–0.01) abrogated MAP kinase activation in the cardiac cells of rats (Fig. 10).

Dox (3 mg/kg) treatment significantly ($p < 0.01$) impeded PI3K/Akt/mTOR signaling in the cardiomyocytes evidenced from the down-regulation in the expressions of PI3K, phospho-Akt and phospho-mTOR in myocardial cells of experimental rats (Fig. 11). On the other hand, oral treatment of ferulic acid (100 mg/kg) or apigenin (100 mg/kg) or WWGPE (100 mg/kg) along with Dox (3 mg/kg) significantly ($p < 0.05$–0.01) reciprocated Dox-mediated impairment of PI3K/Akt/mTOR signaling in the cardiac cells of rats (Fig. 11).

In this study, Dox (3 mg/kg) treatment caused significant ($p < 0.01$) up-regulation of iNOS expression in the heart of rats (Fig. 11). Additionally, significant ($p < 0.01$) down-regulation in the HO-1 and nuclear Nrf-2 expressions was recorded in the myocardial cells of Dox-treated rats (Fig. 11). On the other hand, oral treatment of ferulic acid (100 mg/kg) or apigenin (100 mg/kg) or WWGPE (100 mg/kg) along with Dox (3 mg/kg) significantly ($p < 0.05$–0.01) reciprocated Dox-mediated changes in iNOS, HO-1, and Nrf-2 signaling in the myocardial cells of rats (Fig. 11).

Neither of ferulic acid (100 mg/kg) nor apigenin (100 mg/kg) nor WWGPE (100 mg/kg) could affect in any signal protein expression in myocardial cells when treated alone to the rats (Figs. 9–11).

3.3.4. Effects on the histology of the heart

The histological sections of hearts of rats under different treatments were depicted in Fig. 12. The H & E stained heart section (x 100) of untreated rat revealed normal radiating pattern (yellow arrows). On the other hand, Dox (3 mg/kg) treated rats exhibited the irregular radiating pattern (green arrows) with injured interstitial tissues (red arrows). On the other hand, oral treatment of ferulic acid (100 mg/kg) or apigenin (100 mg/kg) or WWGPE (100 mg/kg) along with Dox (3 mg/kg)

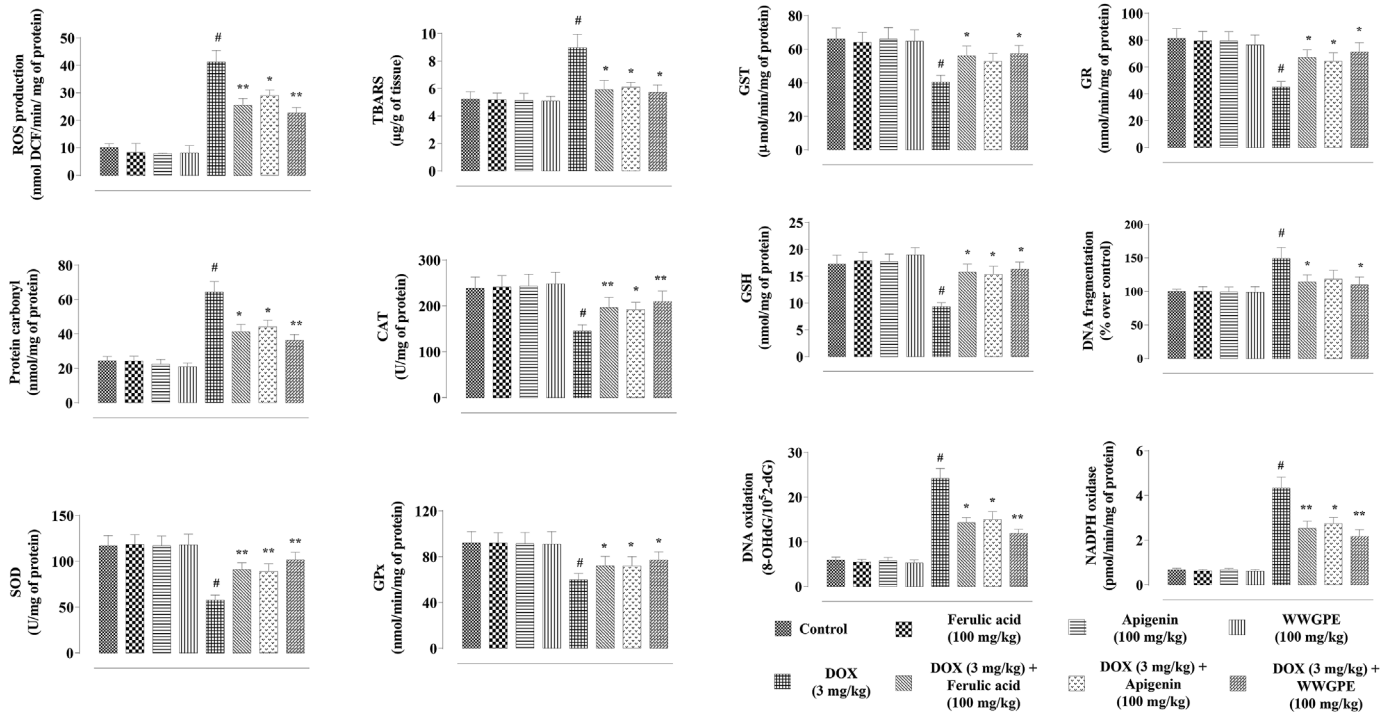

Fig. 8. The effects on ROS accumulation, lipid peroxidation, protein carbonylation, and endogenous redox systems in the absence (Dox) and presence of ferulic acid (Dox + ferulic acid), apigenin (Dox + apigenin), and WWGPE (Dox + WWGPE) *in vivo* in the cardiac tissue of experimental rats. Data were expressed as mean ± SD (n = 3). #Values significantly ($p < 0.01$) differ from normal control. *Values significantly ($p < 0.05$) differ from toxic control. **Values significantly ($p < 0.01$) differ from toxic control. SOD unit, "U", is defined as inhibition (μ moles) of NBT-reduction/min. CAT unit, "U", is defined as H_2O_2 consumption/min.

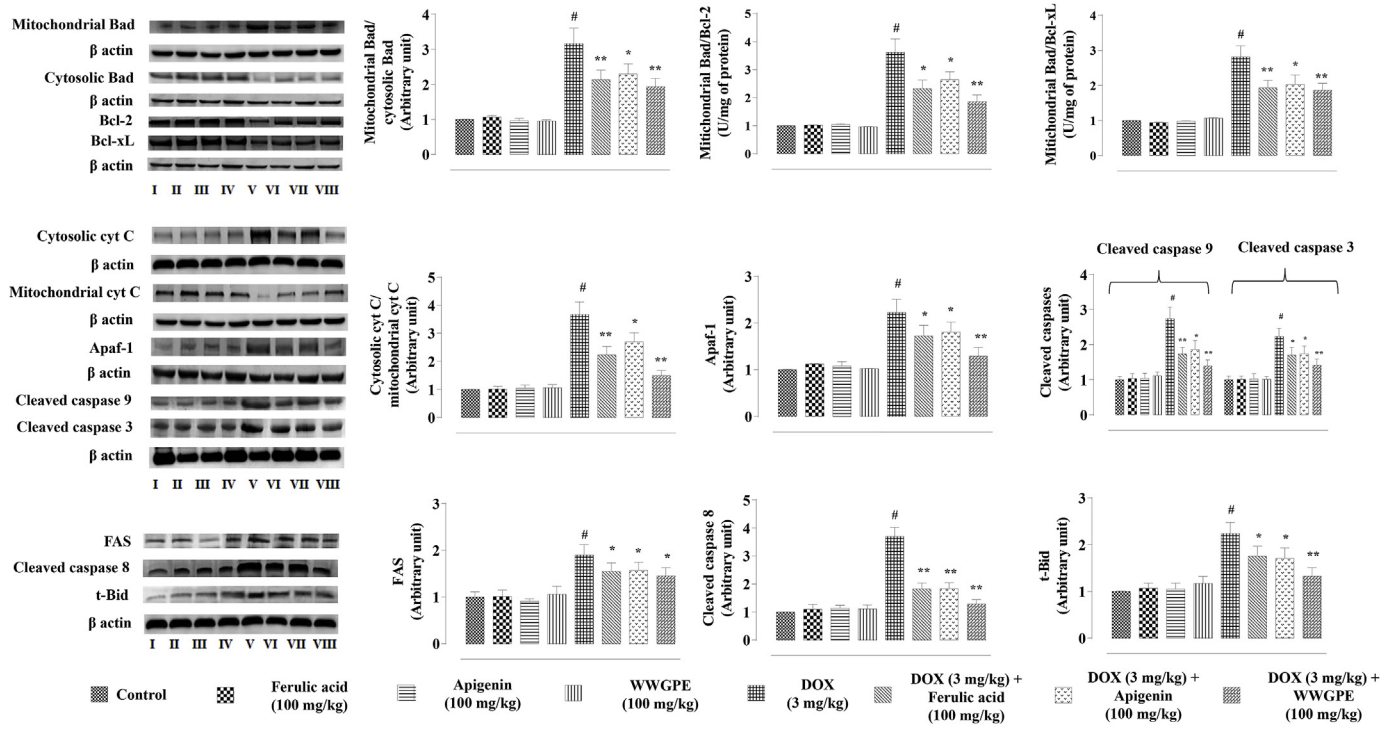

Fig. 9. The effect on intrinsic and extrinsic apoptotic signaling in the absence (Dox) and presence of ferulic acid (Dox + ferulic acid), apigenin (Dox + apigenin), and WWGPE (Dox + WWGPE) *in vivo* in the cardiac cells of experimental rats. The relative band intensities were assessed and the normal control band was allotted a random value of 1. β-actin served as loading control. Data were expressed as mean ± SD (n = 3). #Values significantly ($p < 0.01$) differ from normal control. *Values significantly ($p < 0.05$) differ from toxic control. **Values significantly ($p < 0.01$) differ from toxic control.

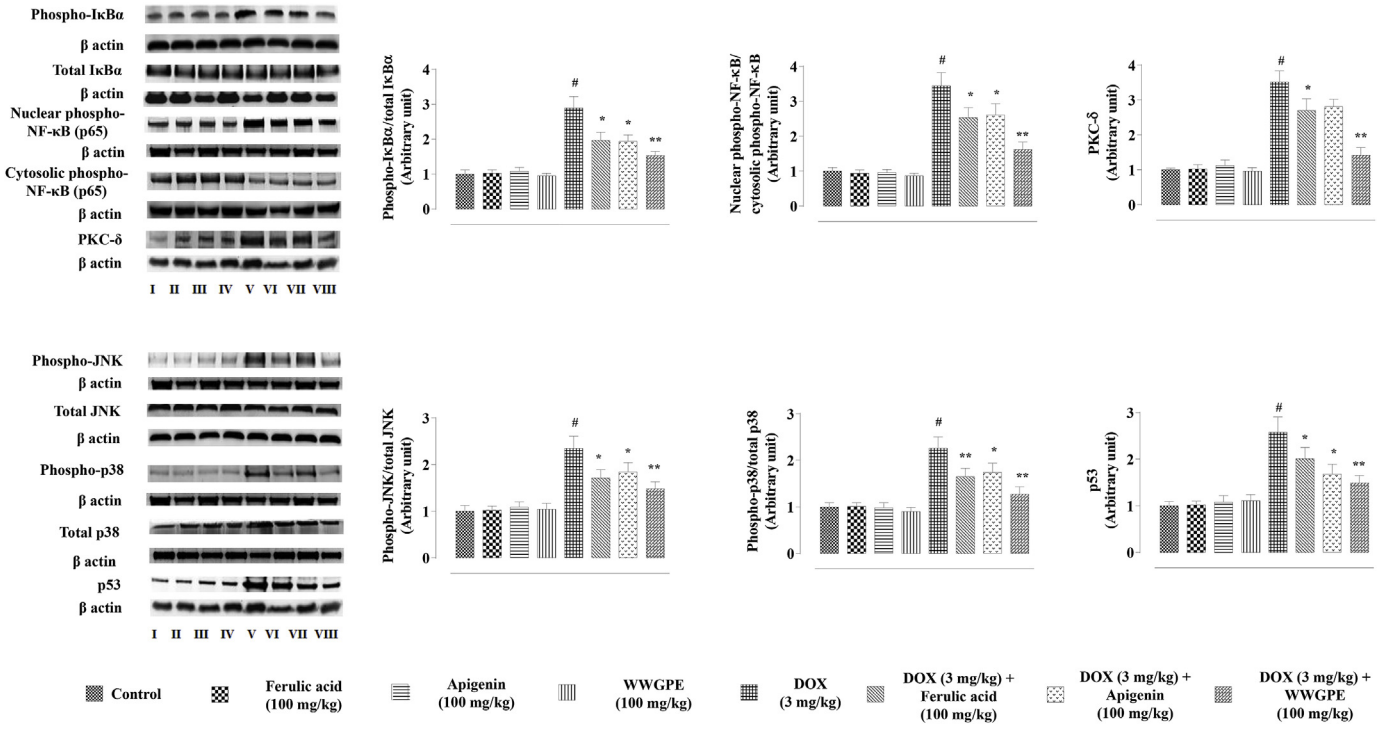

Fig. 10. The effect on IκBα, NF-κB, PKC-δ, JNK, p38, and p53 expressions in the absence (Dox) and presence of ferulic acid (Dox + ferulic acid), apigenin (Dox + apigenin), and WWGPE (Dox + WWGPE) *in vivo* in the cardiac cells of experimental rat. The relative band intensities were assessed and the normal control band was allotted a random value of 1. β-actin served as loading control. Data were expressed as mean ± SD (n = 6). #Values significantly ($p < 0.01$) differ from normal control. *Values significantly ($p < 0.05$) differ from toxic control. **Values significantly ($p < 0.01$) differ from toxic control.

significantly reciprocated the Dox-mediated histological abnormalities and re-established the muscle radiating pattern near to the normal status (Fig. 12). Neither of ferulic acid (100 mg/kg) nor apigenin (100 mg/kg) nor WWGPE (100 mg/kg) could cause any histological change in heart section when treated alone to the rats (Fig. 12).

In *in vivo* study, WWGPE (100 mg/kg) exhibited best protective effect over ferulic acid (100 mg/kg) or apigenin (100 mg/kg) against Dox-induced cardio-toxicity in experimental rats. The order of cardio-protective effect was found to be WWGPE (100 mg/kg) > ferulic acid (100 mg/kg) > apigenin (100 mg/kg) with respect to the all the parameters studied in *in vivo* experiment.

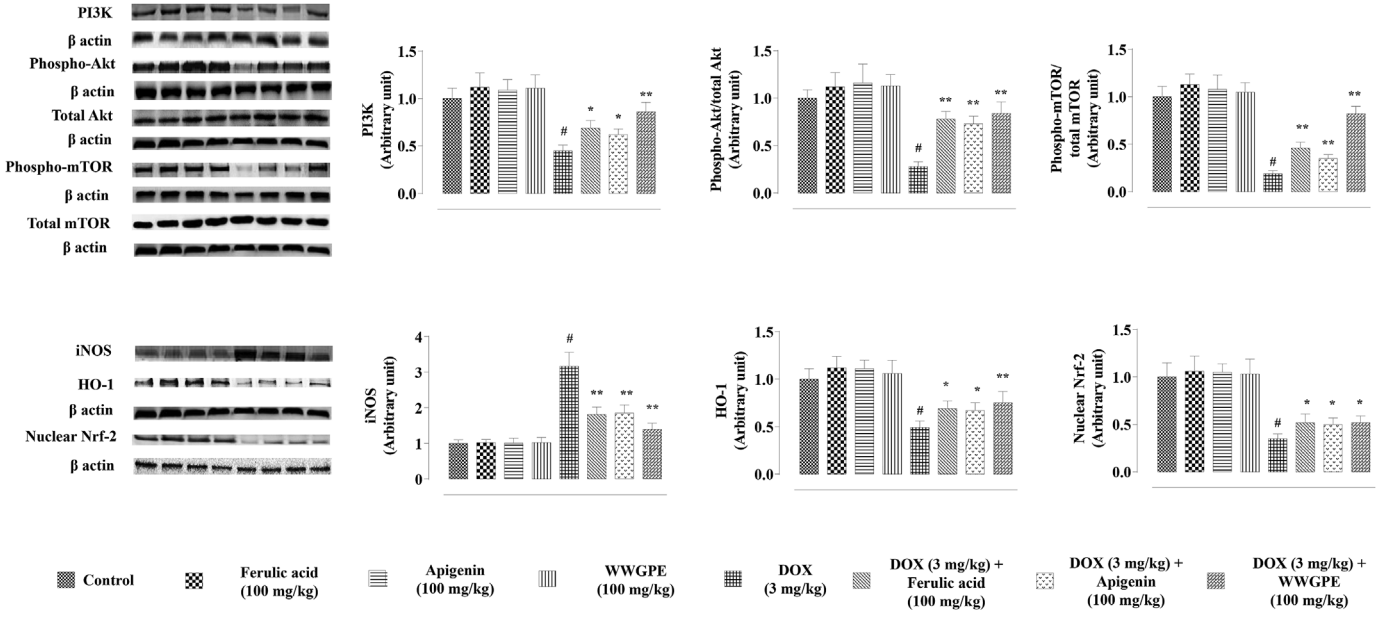

Fig. 11. The effects on PI3K, Akt, mTOR, iNOS, HO-1, and Nrf-2 expressions in the absence (Dox) and presence of ferulic acid (Dox + ferulic acid), apigenin (Dox + apigenin), and WWGPE (Dox + WWGPE) *in vivo* in the cardiac cells of experimental rats. The relative band intensities were assessed and the normal control band was allotted a random value of 1. β-actin served as loading control. Data were expressed as mean ± SD (n = 6). #Values significantly ($p < 0.01$) differ from normal control. *Values significantly ($p < 0.05$) differ from toxic control. Values significantly ($p < 0.01$) differ from toxic control.

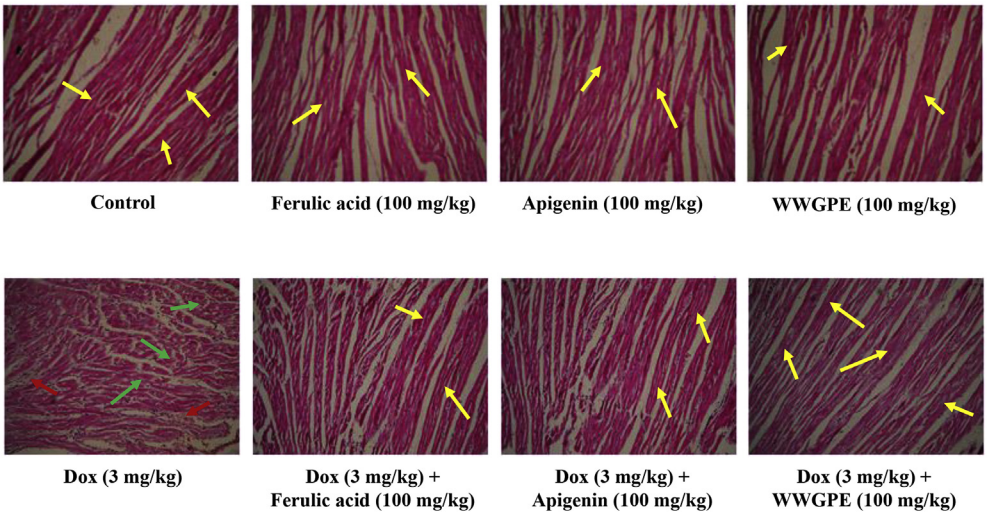

Fig. 12. Histological assessments of hearts of experimental rats in the absence (Dox) and presence of ferulic acid (Dox + ferulic acid), apigenin (Dox + apigenin), and WWGPE (Dox + WWGPE). The H & E stained sections of heart (x 100) of Dox treated rats exhibited the irregular radiating patterns with injured interstitial tissues. Yellow and green arrows denoted normal and irregular radiating patterns, respectively. Red arrows exhibited injured interstitial tissues. On the other hand, treatment with ferulic acid, apigenin, and WWGPE along with Dox restored the radiating patterns of cardiac sections to near-normal status. (For interpretation of the references to color in this figure legend, the reader is referred to the Web version of this article.)

4. Discussion

The adverse effects remain one of the major limitations in the chemotherapy with almost every anti-cancer agent (Dewanjee et al., 2017). Dox is one of the first line chemotherapeutic agents for several malignancies (Chatterjee et al., 2010). However, Dox has been reported to be potential cardio-toxic agent (Chatterjee et al., 2010). It can induce both acute and chronic cardiomyopathy, which can lead to congestive heart failure to the cancer patients (Chatterjee et al., 2010). The proposed etiology of Dox-induced cardiotoxicity includes multiple operative mechanisms (Chatterjee et al., 2010). Enhanced oxidative stress, depletion of endogenous redox defense molecules, induction of cardiac apoptosis, up-regulation of NF-κB/PKC-δ, activation of p53/p38/JNK signaling, and impediment of the PI3K/AKT/mTOR signaling have been proposed to be integrally involved in Dox-mediated cardiomyopathy (Chatterjee et al., 2010; Das et al., 2011; Yu et al., 2017). Plant phenolics are the natural occurring antioxidants, which are reported to attribute a number of cytoprotective mechanisms by neutralizing oxidative free radicals, improving cellular redox defense, and regulating various signal transductions (Dewanjee et al., 2015; Upadhyay and Dixit, 2015; Ávila et al., 2017; Das et al., 2018). Whole wheat grain is a great source of fibers, important minerals, and natural phenolics (Laddomada et al., 2015). Phenolic acids present in wheat bran have been claimed to prevent heart disease via antioxidant mechanism (Laddomada et al., 2015). In addition, bioavailability of wheat grain phenolics as a whole has been claimed to be superior to that of comprising individual phenolic compound in pure form (Gao and Hu, 2010; Laddomada et al., 2015). Considering these, the present study has been undertaken to evaluate protective effect of WWGPE against Dox-induced myocardial toxicity. The cardio-prophylactic effect of WWGPE has been compared with ferulic acid and apigenin, which have been found to be the phenolic acid and the flavonoid present in the WWGPE in highest quantities, respectively.

Haematological and serum biochemical parameters give primary indication of pathological incidence within the body. LDH, CK, and AST levels in the sera serve as diagnostic parameters in cardiomyopathies (Gozalo et al., 2008). These membrane bound enzymes come into the blood during cellular injury (Bhattacharjee et al., 2016). Troponins are considered to be the cardio-specific markers, which release from the myocardial tissues during cardiac injury and ischemia (Kemp et al., 2004). In this study, significant enhancement in the levels of LDH, CK, AST, troponin I, and troponin T indicated establishment of Dox-induced cardiomyopathy to the rats. Besides these, significant changes in serum lipids, haematological counts, and haemoglobin level were observed in Dox-treated rats. On the other hand, ferulic acid or apigenin or WWGPE treatments significantly normalized haematological and serum biochemical parameters, which indicated the probable prophylactic potential of test materials against Dox-mediated myocardial injury.

The data represented herein revealed generation of excessive ROS in the myocardial cells through Dox exposure was responsible to induce oxidative damage, and apoptosis via multiple mechanisms. Mechanism of Dox-meditated ROS production has been yet to be completely understood; however, several mechanisms have been proposed regarding the Dox-mediated ROS generation. Reduction of Dox by mitochondrial electron transport chain generates semiquinone free radicals, which subsequently reduce molecular O_2 to the ROS (Deavall et al., 2012). In this process, NADPH oxidase donates an electron to O_2 for its reduction (Priya et al., 2017). In addition, interaction between Dox and Fe (3) can generate Fe (2)-Dox free radical, which is capable to reduce molecular O_2 to generate ROS (Deavall et al., 2012). ROS can induce oxidative damage to membrane lipids, structural proteins, and nucleic acids (Bhattacharjee et al., 2017). In addition, ROS directly regulate a number of cell signaling pathways resulting cell death (Deavall et al., 2012).

ROS induces peroxidative damage to the cellular lipids (Dewanjee et al., 2017). Dox chemotherapy has been reported to induce cardiotoxicity via peroxidation of myocardial lipids evidenced from enhanced level of lipid conjugated dienes in blood (Minotti et al., 1996). Protein carbonylation via oxidation is an irreversible process of degradation of proteins, which results in cellular dysfunction and disease progression. Earlier study revealed that, Dox can induce cardio-toxicity via oxidative carbonylation of cardiac myosin binding protein (Aryal et al., 2014). In this study, significantly high levels of TBARS, and carbonylated proteins in the myocardial cells following Dox exposure were in the agreement with the earlier observations. Endogenous antioxidant molecules comprising antioxidant enzymes and GSH serve as primary line of cellular defense against oxidative stress (Dewanjee et al., 2009). In this study, Dox caused significant depletion in the levels of SOD, CAT, GST, GPx, GR, and GSH was observed in isolated cardiomyocytes and myocardial tissue. Dox has been reported to be metabolized into doxorubicinol in myocardial cells (Olson et al., 1988). Doxorubicinol can interact with the −SH group of aforementioned antioxidant molecules resulting their inactivation (Dewanjee et al., 2017). Besides, Dox-mediated inactivation of Nrf-2 signaling further caused depletion of aforementioned endogenous antioxidant molecules (Loboda et al., 2016; Barakat et al., 2018). Dox-mediated depletion of endogenous antioxidant enzymes and GSH further enhances the oxidative stress and promotes the progression of cardiomyopathy (Chatterjee et al., 2010; Volkova and Russell, 2011). On the other hand, ferulic acid or apigenin or WWGPE could significantly attenuate Dox-mediated redox stress in cardiac cells. The

antioxidant effect of wheat phenolics was found to be due to the radical scavenging effect coupled with the activation of endogenous antioxidant molecules via activation of Nrf-2 signaling.

ROS can endorse cell death by activating the apoptotic signaling. Dox has been reported to activate p38/JNK/p53 MAP kinase signaling via excessive ROS generation, which can trigger the activation of pro-apoptotic factors and can simultaneously inhibit anti-apoptotic signal proteins, such as Bcl-2, and Bcl-xL (Redza-Dutordoir and Averill-Bates, 2016). In addition, ROS can activate cardiolipin oxidation and increase mitochondrial permeability, which promote cytosolic release of cytochrome *c* from mitochondria and simultaneously trigger caspase signaling in the cytosol through the activation of Apaf-1 (Circu and Aw, 2010; Redza-Dutordoir and Averill-Bates, 2016). ROS can also activate trans-membrane death receptor, such as Fas, which further recruits Fas associated protein with death domain and caspase 8 (Redza-Dutordoir and Averill-Bates, 2016). Cleavage of caspase 8 can promote cleave of Bid to tBid. tBid translocates into mitochondria, where it also stimulates pro-apoptotic factors (Redza-Dutordoir and Averill-Bates, 2016). On the other hand, cleavage of caspase 8 can directly trigger apoptosis via activation of intrinsic caspase signaling. In this study, Dox treatment significantly activated intrinsic and death receptor-mediated apoptosis in the myocardial cells via activation and mitigation pro-apoptotic proteins into mitochondria, down-regulation of anti-apoptotic proteins, cytochrome *c* release into cytosol, activation of transmembrane death receptor, and triggering of caspase signaling. NF-κB signaling is one of the redox sensitive signal transduction, which involves phosphorylation mediated cleavage of NF-κB from its association with inhibitory IκBα in the cytosol and subsequent translocation of phospho−NF−κB into the nucleus, where it activates a number of down-stream signaling cascades (Bhattacharjee et al., 2017; Das et al., 2018). In the nucleus, NF-κB also executes pro-apoptotic factors and impart pro-apoptotic role (Dewanjee et al., 2017). PKC-δ has been reported to activate JNK- and p38- MAP kinases and induces apoptosis (Gonzalez-Guerrico et al., 2005; Panaretakis et al., 2005). In this study, Dox exposure significantly activated NF-κB/PKC-δ signaling. The Dox-mediated generation of excessive ROS may be responsible to the induction of apoptosis to the myocardial cells via regulation of various signal proteins. On the other hand, ferulic acid or apigenin or WWGPE could significantly attenuate Dox-provoked cytotoxic event by reciprocating intrinsic and extrinsic apoptotic signaling, p38/JNK/p53 MAP kinase signaling, and NF-κB/PKC-δ signaling. The anti-apoptotic effect may be correlated to that of ROS scavenging effect of wheat phenolic/s.

Protein kinase B (Akt), a serine/threonine kinase, is the principal signal protein of PI3K/Akt pathway (Das et al., 2011). PI3K/Akt has been reported to promote cell survival by enhancing Mdm2-mediated ubiquitination of p53-MAP kinase (Ogawara et al., 2002). In the present investigation, Dox treatment significantly reduced PI3K and phospho-Akt expressions in myocardial cells with concomitant high expressions of p53 and other pro-apoptotic molecules, which is an indication of reduction of cell survival and induction of apoptosis to the cardiac cells.

The impairment of autophagy has been reported to be a subsidiary mechanism in Dox-induced cardiotoxicity (Yu et al., 2017; Lee et al., 2015). In this study, Dox treatment significantly impeded mTOR phosphorylation, which indicates impairment of autophagy in the myocardial cells. On the other hand, ferulic acid or apigenin or WWGPE could significantly attenuate Dox-provoked impairment in pro-survival and autophagy events by reciprocating PI3K/Akt/mTOR signaling.

Nitric oxide (NO), a potent vasodilator, was found to be involved in the pathogenesis of cardiomyopathy. Dox can elicit cytotoxic effects via NO synthesis in cardiac tissue through activation of iNOS (Boo et al., 2009). iNOS-mediated activation of NO production causes formation of RNS by reacting with superoxide radical, which oxides the cellular macromolecules leading to myocardial redox stress, and apoptosis (Bahadır et al., 2014). Inhibition of iNOS has been found to be beneficial in Dox-mediated cardio-toxicity (Bahadır et al., 2014). In this study, Dox treatment significantly up-regulated iNOS expression in myocardial cells, which was in accordance to the previous report (Pakdeechote et al., 2014). In addition, Dox-mediated ROS generation through NADPH oxidase system participate major role in developing cardiomyopathy via induction of fibrosis, inflammation, and apoptosis (McLaughlin et al., 2017). In this study, Dox treatment caused significant increase in the level of NADPH oxidase in myocardial tissue, which was in accordance to the previous observation (Priya et al., 2017). However, ferulic acid or apigenin or WWGPE treatment significantly reciprocated iNOS and NADPH oxidase activities to near-normal status. Therefore, protective effect of wheat phenolic/s would be correlated to the reduction in the production of oxidative free radicals via inhibition of iNOS and NADPH oxidase activities.

The Nrf-2, a redox-active signal protein, regulates cellular redox balance by up-regulating antioxidant response, and phase 2 detoxification responses in mammals (Loboda et al., 2016). Up-on redox stress, Nrf-2 dissociates from Kelch-like ECH-associated protein 1 (Keap1) in cytosol and translocates into nucleus (Kim et al., 2010). PI3K/Akt signaling has been reported to potentiate Nrf-2 activation (Kim et al., 2010). In nucleus, Nrf-2 binds to the antioxidant responsive element site and leads to the de novo synthesis antioxidant molecules, which efficiently protect cells from oxidative stress (Kim et al., 2010). SOD, GPx, GR, GST, and HO-1 are recognized as some of down-stream signal proteins of Nrf-2 (Loboda et al., 2016). In this study, Dox treatment significantly increased oxidative stress by impeding the activation of Nrf-2, which was in accordance to the previous observation (Barakat et al., 2018). Dox-mediated inactivation of Nrf-2 caused decrease in the levels of endogenous antioxidant enzymes and HO-1 expression in the cardiac cells. On the other hand, ferulic acid or apigenin or WWGPE treatment significantly reciprocated Nrf-2 signaling and up-regulated antioxidant response. Therefore, cardio-protective effect of wheat phenolic/s would be correlated to the reduction of oxidative stress by improving the cellular redox defense system through activation of Nrf-2 signaling.

The chemical structures of the phenolic acids and flavonoids determine their essential reactivity towards oxidative free radicals. Wheat phenolic acids and flavonoids contain multiple −OH groups, which help to scavenge ROS and RNS by direct transferring of protons (Dewanjee et al., 2017). It has been implicated that the radical scavenging effect is proportional to the number of −OH group (Dewanjee et al., 2017). −COOH group can also transfer proton for radical scavenging. Therefore, wheat phenolics may attribute cardio-protective effect via neutralization/scavenging of oxidative free radicals and thereby attenuate Dox-induced myocardial oxidative stress and associated pathological signaling.

In our study, we have observed that, WWGPE offered better cardio-protective effect against Dox-induced cardio-toxicity than ferulic acid and apigenin as observed in *in vitro* and *in vivo* bioassays. In *in vitro* assay, apigenin showed better protection over ferulic acid to the cardiomyocytes against Dox-induced toxicity; while, in *in vivo* bioassay, ferulic acid exhibited better cardio-protection than apigenin. The discrimination between *in vitro* and *in vivo* observations would be due to the difference in the oral bioavailability profiles between ferulic acid and apigenin. Earlier reports advocated that ferulic acid ensured better oral bioavailability then apigenin (Bourne and Rice-Evans, 1998; Adam et al., 2002; Ding et al., 2014). On the other hand, WWGPE exhibited better cardio-protective effect then both the compounds. Earlier report revealed that antioxidant power of phenolic compounds largely depends on the number of hydroxyl group (Dewanjee et al., 2017). Clearly, WWGPE represents more hydroxyl groups than individual phenolic components, which would be the reason of synergy of the comprising phenolic acids and flavonoids to exhibit better protective effect against xenobiotic-mediated oxidative stress. In addition, oral bioavailability of wheat grain phenolics has been implicated to be superior when consumed as a whole to that of comprising individual phenolic compound (Sahu et al., 2016; Gao and Hu, 2010).

In conclusion, the present study implicated that the polyphenolic

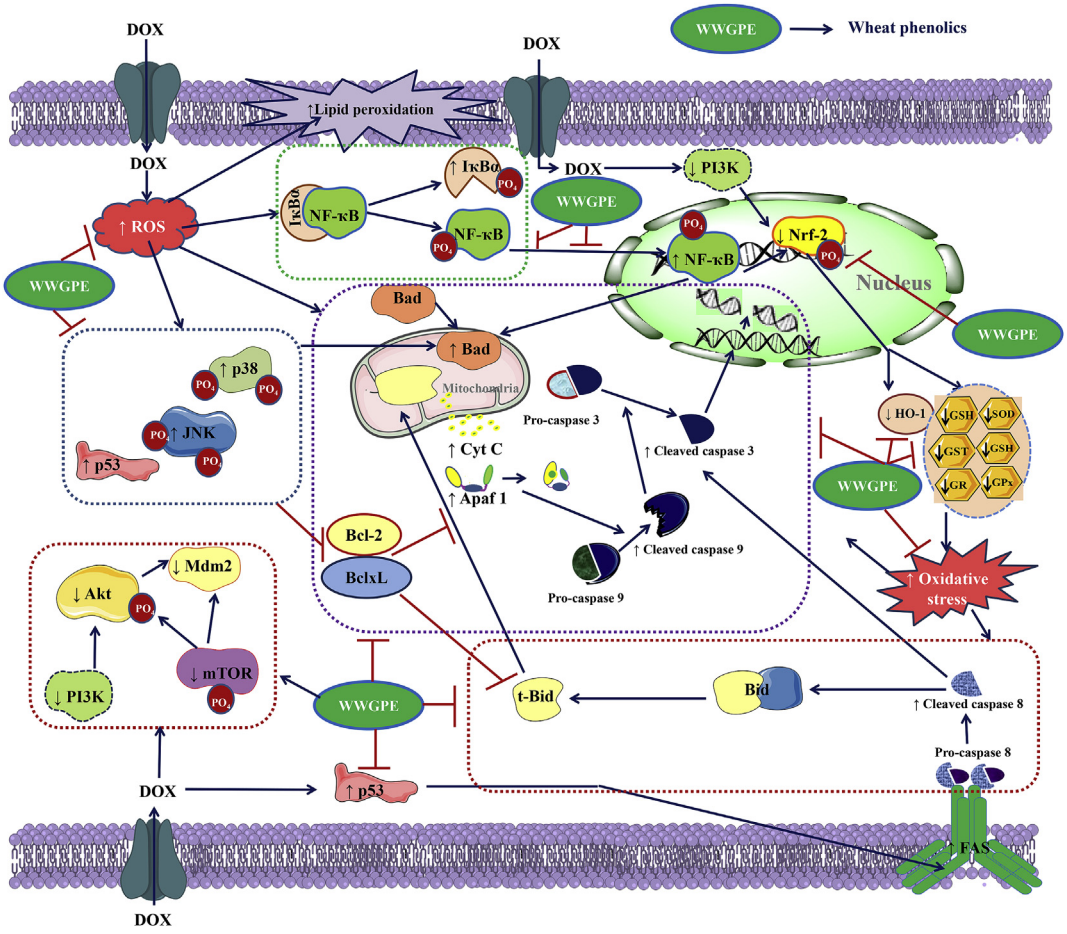

Fig. 13. Schematic overview of established protective mechanism of WWGPE against DOX-mediated myocardial injury. The blue arrows indicated down-steam cellular events. The red lines indicated the activities restricted. (For interpretation of the references to color in this figure legend, the reader is referred to the Web version of this article.)

extract of whole wheat grains is a rich source of naturally occurring antioxidant molecules, which play a potential role to combat against Dox-induced cardio-toxicity by inhibiting oxidative stress, MAP kinase activation, NF-κB pathway, PI3K/Akt/mTOR impairment, and apoptosis in the Dox-exposed myocardial cells (Fig. 13). Results further implicated that, polyphenolic extract of whole wheat grains offered better cardio-protective effect than ferulic acid and apigenin, which were found to be most abundant phenolic acid and flavonoid in the polyphenolic extract, respectively. Combining all, it would be accentuated that supplementation of whole wheat grain polyphenolics could ameliorate cardio-toxic adverse effect of Dox during Dox-chemotherapy.

Authors' contribution

SD and VDF designed the experiments. RS and TKD performed the *in vitro* assays and subsequent analyses. RS, TKD, and SDas, performed *in vivo* assay and subsequent analyses. SD and VDF compiled and analyzed the data. SD and VDF wrote the manuscript.

Conflicts of interest

None.

Acknowledgments

Council of Scientific & Industrial Research (CSIR), New Delhi, India is acknowledged for awarding research project (Ref. No. 02(0275)/16/EMR-II dated 06.12.2016) to Dr. Saikat Dewanjee. Authors are grateful to University Grants Commission (UGC), New Delhi, for providing the financial assistance to Dr. Ranabir Sahu (Ref. no. No. F./PDFSS-2013-14-ST-WES-6992) and Mr. Sonjit Das (Ref. no. F1-17.1/2013-14/RGNF-2013-14-SC-ASS-52029 (SA-III/Website)). Finally, authors are thankful to Jadavpur University, Kolkata, India and University of Salerno, Salerno, Italy for their sincere supports.

Appendix A. Supplementary data

Supplementary data to this article can be found online at https://doi.org/10.1016/j.fct.2019.01.034.

Transparency document

Transparency document related to this article can be found online at https://doi.org/10.1016/j.fct.2019.01.034.

References

Adam, A., Crespy, V., Levrat-Verny, M.-A., Leenhardt, F., Leuillet, M., Demigné, C., Rémésy, C., 2002. The bioavailability of ferulic acid is governed primarily by the food matrix rather than its metabolism in intestine and liver in rats. J. Nutr. 132 (7), 1962–1968.

Aryal, B., Jeong, J., Rao, V.A., 2014. Doxorubicin-induced carbonylation and degradation of cardiac myosin binding protein C promote cardiotoxicity. Proc. Natl. Acad. Sci. Unit. States Am. 111 (5), 2011–2016.

Ávila, F., Theoduloz, C., López-Alarcón, C., Dorta, E., Schmeda-Hirschmann, G., 2017. Cytoprotective mechanisms mediated by polyphenols from Chilean native berries against free radical-induced damage on AGS cells. Oxid. Med. Cell. Longev. 9808520. 2017. https://doi.org/10.1155/2017/9808520.

Baghirova, S., Hughes, B.G., Hendzel, M.J., Schulz, R., 2015. Sequential fractionation and isolation of subcellular proteins from tissue or cultured cells. MethodsX 2, 440–445.
Bahadır, A., Kurucu, N., Kadıoğlu, M., Yenilme, E., 2014. The role of nitric oxide in doxorubicin-induced cardiotoxicity: experimental study. Turk. J. Hematol. 31 (1), 68–74.
Barakat, B.M., Ahmed, H.I., Bahr, H.I., Elbahaie, A.M., 2018. Protective effect of boswellic acids against doxorubicin-induced hepatotoxicity: impact on Nrf2/HO-1 defense pathway. Oxid. Med. Cell. Longev. 8296451. 2018. https://doi.org/10.1155/2018/8296451.
Bhattacharjee, N., Dua, T.K., Khanra, R., Joardar, S., Nandy, A., Saha, A., De Feo, V., Dewanjee, S., 2017. Protocatechuic acid, a phenolic from *Sansevieria roxburghiana* leaves, suppresses diabetic cardiomyopathy via stimulating glucose metabolism, ameliorating oxidative stress, and inhibiting inflammation. Front. Pharmacol. 8, 251. https://doi.org/10.3389/fphar.2017.00251.
Bhattacharjee, N., Khanra, R., Dua, T.K., Das, S., De, B., Zia-Ul-Haq, M., De Feo, V., Dewanjee, S., 2016. *Sansevieria roxburghiana* Schult. & Schult. F. (Family: Asparagaceae) attenuates type 2 diabetes and its associated cardiomyopathy. PLoS One 11 e0167131. https://doi.org/10.1371/journal.pone.0167131.
Boo, S.D., Kopecka, J., Brusa, D., Gazzano, E., Matera, L., Ghigo, D., Bosia, A., Riganti, C., 2009. iNOS activity is necessary for the cytotoxic and immunogenic effects of doxorubicin in human colon cancer cells. Mol. Canc. 8 (108). https://doi.org/10.1186/1476-4598-8-108.
Bourne, L.C., Rice-Evans, C., 1998. Bioavailability of ferulic acid. Biochem. Biophys. Res. Commun. 253 (2), 222–227.
Carvalho, F.S., Burgeiro, A., Garcia, R., Moreno, A.J., Carvalho, R.A., Oliveira, P.J., 2014. Doxorubicin-induced cardiotoxicity: from bioenergetic failure and cell death to cardiomyopathy. Med. Res. Rev. 34 (1), 106–135.
Chatterjee, K., Zhang, J., Honbo, N., Karliner, J.S., 2010. Doxorubicin cardiomyopathy. Cardiology 115 (2), 155–162.
Circu, M.L., Aw, T.Y., 2010. Reactive oxygen species, cellular redox systems, and apoptosis. Free Radic. Biol. Med. 48 (6), 749–762.
Das, J., Ghosh, J., Manna, P., Sil, P.C., 2011. Taurine suppresses doxorubicin-triggered oxidative stress and cardiac apoptosis in rat via up-regulation of PI3-K/Akt and inhibition of p53, p38-JNK. Biochem. Pharmacol. 81 (7), 891–909.
Das, S., Joardar, S., Manna, P., Dua, T.K., Bhattacharjee, N., Khanra, R., Bhowmick, S., Kalita, J., Saha, A., Ray, S., De Feo, V., 2018. Carnosic Acid, a natural diterpene, attenuates arsenic-induced hepatotoxicity via reducing oxidative stress, MAPK activation, and apoptotic cell death pathway. Oxid. Med. Cell. Longev. 1421438. 2018. https://doi.org/10.1155/2018/1421438.
Deavall, D.G., Martin, E.A., Horner, J.M., Roberts, R., 2012. Drug-induced oxidative stress and toxicity. J. Toxicol. 645460. 2012. https://doi.org/10.1155/2012/645460.
Dewanjee, S., Das, A.K., Sahu, R., Gangopadhyay, M., 2009. Antidiabetic activity of *Diospyros peregrina* fruit: effect on hyperglycemia, hyperlipidemia and augmented oxidative stress in experimental type 2 diabetes. Food Chem. Toxicol. 47 (10), 2679–2685.
Dewanjee, S., Das, S., Das, A.K., Bhattacharjee, N., Dihingia, A., Dua, T.K., Kalita, J., Manna, P., 2018. Molecular mechanism of diabetic neuropathy and its pharmacotherapeutic targets. Eur. J. Pharmacol. 833, 472–523.
Dewanjee, S., Dua, T.K., Khanra, R., Das, S., Barma, S., Joardar, S., Bhattacharjee, N., Zia-Ul-Haq, M., Jaafar, H.Z., 2015. Water spinach, *Ipomoea aquatica* (Convolvulaceae), ameliorates lead toxicity by inhibiting oxidative stress and apoptosis. PLoS One 10, e0139831. https://doi.org/10.1371/journal.pone.0139831.
Dewanjee, S., Joardar, S., Bhattacharjee, N., Dua, T.K., Das, S., Kalita, J., Manna, P., 2017. Edible leaf extract of *Ipomoea aquatica* Forssk. (Convolvulaceae) attenuates doxorubicin-induced liver injury via inhibiting oxidative impairment, MAPK activation and intrinsic pathway of apoptosis. Food Chem. Toxicol. 105, 322–336.
Dewanjee, S., Sahu, R., Karmakar, S., Gangopadhyay, M., 2013. Toxic effects of lead exposure in Wistar rats: involvement of oxidative stress and the beneficial role of edible jute (*Corchorus olitorius*) leaves. Food Chem. Toxicol. 55, 78–91.
Ding, S.M., Zhang, Z.H., Song, J., Cheng, X.D., Jiang, J., Jia, X.B., 2014. Enhanced bioavailability of apigenin via preparation of a carbon nanopowder solid dispersion. Int. J. Nanomed. 9 (1), 2327–2333.
Dua, T.K., Dewanjee, S., Gangopadhyay, M., Khanra, R., Zia-Ul-Haq, M., De Feo, V., 2015. Ameliorative effect of water spinach, *Ipomea aquatica* (Convolvulaceae), against experimentally induced arsenic toxicity. J. Transl. Med. 13 (1), 81. https://doi.org/10.1186/s12967-015-0430-3.
Dua, T.K., Dewanjee, S., Khanra, R., 2016. Prophylactic role of *Enhydra fluctuans* against arsenic-induced hepatotoxicity via anti-apoptotic and antioxidant mechanisms. Redox Rep. 21, 147–154.
Fraga, C.G., Leibovita, B.E., Toppel, A.L., 1988. Lipid peroxidation measured as TBARS in tissue slices: characterisation and comparison with homogenates and microsomes. Free Radic. Biol. Med. 4, 155–161.
Gao, S., Hu, M., 2010. Bioavailability challenges associated with development of anti-cancer phenolics. Mini Rev. Med. Chem. 10, 550–567.
Ghosh, J., Das, J., Manna, P., Sil, P.C., 2011. The protective role of arjunolic acid against doxorubicin induced intracellular ROS dependent JNK-p38 and p53-mediated cardiac apoptosis. Biomaterials 32 (21), 4857–4866.
Gonzalez-Guerrico, A.M., Meshki, J., Xiao, L., Benavides, F., Conti, C.J., Kazanietz, M.G., 2005. Molecular mechanisms of protein kinase C-induced apoptosis in prostate cancer cells. J. Biochem. Mol. Biol. 38 (6), 639–645.
Gozalo, A.S., Chavera, A., Montoya, E.J., Takano, J., Weller, R.E., 2008. Relationship of creatine kinase, aspartate aminotransferase, lactate dehydrogenase, and proteinuria to cardiomyopathy in the owl monkey (*Aotus vociferans*). J. Med. Primatol. 37, 29–38.
Gupta, V.K., Sharma, B., 2017. Role of phytochemicals in neurotrophins mediated regulation of Alzheimer's disease. Int. J. Complement. Alt. Med. 7https://doi.org/10.15406/ijcam.2017.07.00231. 00231.
Gupta, V.K., Sharma, B., 2018. Phytochemicals from Indian traditional plants as natural potential therapeutic agents against adenosquamous lungs. Pharmacologia 9, 39–45.
Gupta, V.K., Singh, R., Sharma, B., 2017. Phytochemicals mediated signaling pathways and their implications in cancer chemotherapy: challenges and opportunities in phytochemicals based drug development: a review. Biochem. Compd. 5, 1–15.
Gupta, V.K., Singh, S., Agrawal, A., Siddiqi, N.J., Sharma, B., 2015. Phytochemicals mediated remediation of neurotoxicity induced by heavy metals. Biochem. Res. Int. https://doi.org/10.1155/2015/534769. 2015, Article ID 534769.
Injac, R., Strukelj, B., 2008. Recent advances in protection against doxorubicin-induced toxicity. Technol. Canc. Res. Treat. 7 (6), 497–516.
Kemp, M., Donovan, J., Higham, H., Hooper, J., 2004. Biochemical markers of myocardial injury. Br. J. Anaesth. 93 (1), 63–73.
Kim, K.C., Kang, K.A., Zhang, R., Piao, M.J., Kim, G.Y., Kang, M.Y., Lee, S.J., Lee, N.H., Surh, Y.J., Hyun, J.W., 2010. Up-regulation of Nrf2-mediated heme oxygenase-1 expression by eckol, a phlorotannin compound, through activation of Erk and PI3K/Akt. Int. J. Biochem. Cell Biol. 42 (2), 297–305.
Laddomada, B., Caretto, S., Mita, G., 2015. Wheat bran phenolic acids: bioavailability and stability in whole wheat-based foods. Molecules 20 (9), 15666–15685.
Lee, B.S., Oh, J., Kang, S.K., Park, S., Lee, S.-H., Choi, D., Chung, J.H., Chung, Y.W., Kang, S.-M., 2015. Insulin protects cardiac myocytes from doxorubicin toxicity by Sp1-mediated transactivation of survivin. PLoS One 10 (8), e0135438. https://doi.org/10.1371/journal.pone.0135438.
Loboda, A., Damulewicz, M., Pyza, E., Jozkowicz, A., Dulak, J., 2016. Role of Nrf2/HO-1 system in development, oxidative stress response and diseases: an evolutionarily conserved mechanism. Cell. Mol. Life Sci. 73, 3221–3247.
Manna, P., Jain, S.K., 2013. L-cysteine and hydrogen sulfide increase PIP3 and AMPK/PPARγ expression and decrease ROS and vascular inflammation markers in high glucose treated human U937 monocytes. J. Cell. Biochem. 114 (10), 2334–2345.
Manna, P., Sinha, M., Sil, P.C., 2009. Protective role of arjunolic acid in response to streptozotocin-induced type-I diabetes via the mitochondrial dependent and independent pathways. Toxicology 257 (1–2), 53–63.
McLaughlin, D., Zhao, Y., O'neill, K.M., Edgar, K.S., Dunne, P.D., Kearney, A.M., Grieve, D.J., McDermott, B.J., 2017. Signalling mechanisms underlying doxorubicin and Nox2 NADPH oxidase-induced cardiomyopathy: involvement of mitofusin-2. Br. J. Pharmacol. 174 (21), 3677–3695.
Minotti, G., Mancuso, C., Frustaci, A., Mordente, A., Santini, S.A., Calafiore, A.M., Liberi, G., Gentiloni, N., 1996. Paradoxical inhibition of cardiac lipid peroxidation in cancer patients treated with doxorubicin. Pharmacologic and molecular reappraisal of anthracycline cardiotoxicity. J. Clin. Invest. 98 (3), 650–661.
Ogawara, Y., Kishishita, S., Obata, T., Isazawa, Y., Suzuki, T., Tanaka, K., Masuyama, N., Gotoh, Y., 2002. Akt enhances Mdm2-mediated ubiquitination and degradation of p53. J. Biol. Chem. 277 (24), 21843–21850.
Olson, R.D., Mushlin, P.S., Brenner, D.E., Fleischer, S., Cusack, B.J., Chang, B.K., Boucek, R.J., 1988. Doxorubicin cardiotoxicity may be caused by its metabolite, doxorubicinol. Proc. Natl. Acad. Sci. Unit. States Am. 85, 3585–3589.
Pakdeechote, P., Bunbupha, S., Kukongviriyapan, U., Prachaney, P., Khrisanapant, W., Kukongviriyapan, V., 2014. Asiatic acid alleviates hemodynamic and metabolic alterations via restoring eNOS/iNOS expression, oxidative stress, and inflammation in diet-induced metabolic syndrome rats. Nutrients 6 (1), 355–370.
Panaretakis, T., Laane, E., Pokrovskaja, K., Bjorklund, A.-C., Moustakas, A., Zhivotovsky, B., Heyman, M., Shoshan, M.C., Grandér, D., 2005. Doxorubicin requires the sequential activation of caspase-2, protein kinase Cδ, and c-Jun NH2-terminal kinase to induce apoptosis. Mol. Biol. Cell 16 (8), 3821–3831.
Pandey, K.B., Rizvi, S.I., 2009. Plant polyphenols as dietary antioxidants in human health and disease. Oxid. Med. Cell. Longev. 2, 270–278.
Priya, L.B., Baskaran, R., Huang, C.Y., Padma, V.V., 2017. Neferine ameliorates cardiomyoblast apoptosis induced by doxorubicin: possible role in modulating NADPH oxidase/ROS-mediated NFκB redox signaling cascade. Sci. Rep. 7 (1), 12283. https://doi.org/10.1038/s41598-017-12060-9.
Public Health Service (PHS), 2015. Public Health Service Policy on Human Care and Use of Laboratory Animals. US Department of Health and Human Services, National Institute of Health, Office of Laboratory Animal welfare, Washington, DC.
Redza-Dutordoir, M., Averill-Bates, D.A., 2016. Activation of apoptosis signalling pathways by reactive oxygen species. Biochim. Biophys. Acta 1863 (12), 2977–2992.
Sahu, R., Sharaff, M., Pradhan, M., Sethi, A., Bandyopadhyay, T., Mishra, V.K., Chand, R., Chowdhury, A.K., Joshi, A.K., Pandey, S.P., 2016. Elucidation of defense-related signaling responses to spot blotch infection in bread wheat (*Triticum aestivum* L.). Plant J. 86 (1), 35–49.
Sharma, B., Gupta, V.K., 2016. Modulations of mammalian brain functions by antidepressant drugs: role of some phytochemicals as prospective antidepressants. Evid. Based Med. Pract. 2https://doi.org/10.4172/ebmp.1000003. 003.
Singh, N., Sharma, B., 2018. Biotoxins mediated DNA damage and role of phytochemicals in DNA protection. ˙ Biochem. Mol. Biol. J. 4https://doi.org/10.21767/2471-8084.100054. 1:5.
Takemura, G., Fujiwara, H., 2007. Doxorubicin-induced cardiomyopathy: from the cardiotoxic mechanisms to management. Prog. Cardiovasc. Dis. 49 (5), 330–352.
Uchida, K., Stadtman, E.R., 1993. Covalent attachment of 4-hydroxynonenal to glyceraldehydes- 3-phosphate dehydrogenase. J. Biol. Chem. 268, 6388–6393.
Upadhyay, S., Dixit, M., 2015. Role of polyphenols and other phytochemicals on molecular signaling. Oxid. Med. Cell. Longev. 504253. 2015. https://doi.org/10.1155/2015/504253.
Volkova, M., Russell, R., 2011. Anthracycline cardiotoxicity: prevalence, pathogenesis and treatment. Curr. Cardiol. Rev. 7 (4), 214–220.
Wardyn, J.D., Ponsford, A.H., Sanderson, C.M., 2015. Dissecting molecular cross-talk between Nrf2 and NF-κB response pathways. Biochem. Soc. Trans. 43 (4), 621–626.
Yu, W., Sun, H., Zha, W., Cui, W., Xu, L., Min, Q., Wu, J., 2017. Apigenin attenuates adriamycin-induced cardiomyocyte apoptosis via the PI3K/AKT/mTOR pathway. Evid. Based Complement. Alternat. Med. 2590676. 2017. https://doi.org/10.1155/2017/2590676.